Properties of a Novel pH-dependent Ca^{2+} Permeation Pathway Present in Male Germ Cells with Possible Roles in Spermatogenesis and Mature Sperm Function

Celia M. Santi,*‡ Teresa Santos,* Arturo Hernández-Cruz,* and Alberto Darszon*

From the *Departamento de Biofísica, Instituto de Fisiología Celular, Universidad Nacional Autónoma de México, Circuito Exterior, Ciudad Universitaria México City, D.F. 04510, México; and ‡Departamento de Genética y Fisiología Molecular, Instituto de Biotecnología, Universidad Nacional Autónoma de México, Cuernavaca, Morelos 62271, México

ABSTRACT Rises of intracellular Ca^{2+} ($[Ca^{2+}]_i$) are key signals for cell division, differentiation, and maturation. Similarly, they are likely to be important for the unique processes of meiosis and spermatogenesis, carried out exclusively by male germ cells. In addition, elevations of $[Ca^{2+}]_i$ and intracellular pH (pH_i) in mature sperm trigger at least two events obligatory for fertilization: capacitation and acrosome reaction. Evidence implicates the activity of Ca^{2+} channels modulated by pH_i in the origin of these Ca^{2+} elevations, but their nature remains unexplored, in part because work in individual spermatozoa are hampered by formidable experimental difficulties. Recently, late spermatogenic cells have emerged as a model system for studying aspects relevant for sperm physiology, such as plasmalemmal ion fluxes. Here we describe the first study on the influence of controlled intracellular alkalinization on $[Ca^{2+}]_i$ on identified spermatogenic cells from mouse adult testes. In BCECF [(2′,7′)-bis(carboxymethyl)-(5,6)-carboxyfluorescein]-AM-loaded spermatogenic cells, a brief (30–60 s) application of 25 mM NH_4Cl increased pH_i by ~1.3 U from a resting pH_i ~6.65. A steady pH_i plateau was maintained during NH_4Cl application, with little or no rebound acidification. In fura-2-AM-loaded cells, alkalinization induced a biphasic response composed of an initial $[Ca^{2+}]_i$ drop followed by a two- to threefold rise. Maneuvers that inhibit either Ca^{2+} influx or intracellular Ca^{2+} release demonstrated that the majority of the Ca^{2+} rise results from plasma membrane Ca^{2+} influx, although a small component likely to result from intracellular Ca^{2+} release was occasionally observed. Ca^{2+} transients potentiated with repeated NH_4Cl applications, gradually obliterating the initial $[Ca^{2+}]_i$ drop. The pH-sensitive Ca^{2+} permeation pathway allows the passage of other divalents (Sr^{2+}, Ba^{2+}, and Mn^{2+}) and is blocked by inorganic Ca^{2+} channel blockers (Ni^{2+} and Cd^{2+}), but not by the organic blocker nifedipine. The magnitude of these Ca^{2+} transients increased as maturation advanced, with the largest responses being recorded in testicular sperm. By extrapolation, these findings suggest that the pH-dependent Ca^{2+} influx pathway could play significant roles in mature sperm physiology. Its pharmacology and ion selectivity suggests that it corresponds to an ion channel different from the voltage-gated T-type Ca^{2+} channel also present in spermatogenic cells. We postulate that the Ca^{2+} permeation pathway regulated by pH_i, if present in mature sperm, may be responsible for the dihydropyridine-insensitive Ca^{2+} influx required for initiating the acrosome reaction and perhaps other important sperm functions.

KEY WORDS: calcium signaling • calcium entry • pH regulation • sperm physiology • spermatogenesis

INTRODUCTION

Spermatogenesis is a complex and highly coordinated process by which spermatogonia proliferate and differentiate to produce mature sperm. This unique process depends on the capacity of spermatogonia to undergo proliferation and to enter into a differentiation program that includes a meiotic cycle. There is ample evidence indicating that elevations of intracellular Ca^{2+} concentration ($[Ca^{2+}]_i$) are key signals for cell division, differentiation, and maturation of somatic cells. Thus, $[Ca^{2+}]_i$ may be important for spermatogenesis, although very little is known about its regulation in spermatogenic cells (reviewed in Jegou, 1993). An important step towards understanding germ cell $[Ca^{2+}]_i$ regulation was the demonstration that T-type Ca^{2+} channels constitute their only voltage-gated Ca^{2+} permeation pathway (Arnoult et al., 1996*b*; Liévano et al., 1996; Santi et al., 1996). These channels, either alone or in combination with other Ca^{2+} signaling mechanisms, could play important roles in spermatogenesis (Santi et al., 1996).

Significantly more data exist in the role of $[Ca^{2+}]_i$ variations in mature sperm, although a universally accepted model has yet to be published. Changes in intra-

Drs. Hernández-Cruz and Darszon contributed equally to this article.

Portions of this work were previously published in abstract form (Santi, C.M., A. Darszon, and A. Hernández-Cruz. 1997. *Biophys. J.* 72: *a*34).

Address correspondence to Celia M. Santi, M.D., Departamento de Biofísica, Instituto de Fisiología Celular, UNAM, Circuito Exterior, Ciudad Universitaria, México City, D.F. 04510, P.O. Box 70-253, México. Fax: 525-622-56-07; E-mail: cgrau@ifcsun1.ifisiol.unam.mx

cellular pH (pH_i) and $[Ca^{2+}]_i$ in mammalian sperm have been implicated in the control of capacitation and the acrosome reaction (AR),[1] a Ca^{2+}-dependent exocytotic event required for fertilization. Evidence suggests that a Ca^{2+} channel modulated by pH_i also participates in the sea urchin sperm AR (García-Soto et al., 1987; Guerrero and Darszon, 1989*a*). The nature of the membrane events of this activation pathway is not clear yet, nor is it well understood how internal alkalinization can induce the elevation of intracellular Ca^{2+} required for the physiological response (Florman et al., 1989; Florman, 1994; Arnoult et al., 1996*a*).

A close interrelationship between pH_i and $[Ca^{2+}]_i$ has been demonstrated in a variety of somatic cell types. In particular, cytosolic alkalinization modestly increases $[Ca^{2+}]_i$ in cultured smooth muscle cells (Siskind et al., 1989), endothelial cells (Danthuluri et al., 1990), HT_{29} colon carcinoma cells (Benning et al., 1996; Nitschke et al., 1996), rat lachrymal acinar cells (Yodozawa et al., 1997), rat lymphocytes (Grinstein and Goetz, 1985), and several neuronal or neuroendocrine cell types (Dickens et al., 1990; Shorte et al., 1991).

The $[Ca^{2+}]_i$ changes induced when ZP3 (a glycoprotein of the egg's zona pellucida) binds to its receptor on the sperm membrane have been recorded in fura-2-loaded bovine and mouse sperm (Florman, 1994; Arnoult et al., 1996*a*). However, the minute volume of these cells makes reliable detection of fura-2 fluorescence difficult and electrophysiology very arduous (Darszon et al., 1996). Using mouse spermatogenic cells can circumvent some of these obstacles. Their large volume improves signal to noise ratio of fluorescence measurements. Also, recordings of ionic currents are much simpler than in sperm (Santi et al., 1996; Arnoult et al., 1996*b*), and it is possible to apply strategies of molecular biology to learn about their ion channel composition (Liévano et al., 1996). Late spermatogenic cells can be considered a suitable approximation to mature sperm since they possess many of the membrane proteins present in these transcriptionally inactive, terminal cells (Hetch, 1988).

This study was designed to evaluate the influence of changes in pH_i on $[Ca^{2+}]_i$ homeostasis of spermatogenic cells from adult male mice. Our main goal was to determine if cytosolic alkalinization, elicited by the controlled exposure to a permeant weak base, induces changes in $[Ca^{2+}]_i$ and, if so, to understand the mechanism by which these changes occur. Furthermore, by taking advantage of the fact that cells from different stages of spermatogenesis and spermiogenesis can be readily identified, their individual responses to intracellular alkalinization were examined and compared.

Our results indicate that internal alkalinization consistently induces Ca^{2+} transients. Using maneuvers that inhibit plasmalemmal Ca^{2+} influx or Ca^{2+} release from internal stores, we concluded that the majority of Ca^{2+} rise results from plasmalemmal Ca^{2+} influx, although a small component that could be attributed to intracellular Ca^{2+} release was occasionally observed. The alkalinization-induced Ca^{2+} permeation pathway allows the passage of other divalents such as Sr^{2+}, Ba^{2+}, and Mn^{2+}. In addition, the inorganic Ca^{2+} channel blockers Ni^{2+} and Cd^{2+} block this Ca^{2+} influx pathway, but not the organic blocker nifedipine. The pharmacological properties of this Ca^{2+} influx pathway virtually rule out a major contribution of voltage-gated Ca^{2+} channels or the Na^+/Ca^{2+} exchanger.

The magnitude of the Ca^{2+} elevations increases as maturation advances, suggesting a significant role of this mechanism in sperm physiology. We postulate that this novel Ca^{2+} permeation pathway regulated by intracellular pH may contribute, in combination with voltage-gated Ca^{2+} channels, to support Ca^{2+} signals required for spermatogenesis and spermiogenesis. Also, if present in mature sperm, it could be involved in the generation of Ca^{2+} signals needed to initiate important functions such as capacitation and acrosome reaction.

MATERIALS AND METHODS

Dissociation Procedure

Spermatogenic cells were obtained as in Santi et al. (1996). Briefly, decapsulated testes of adult male mice (anesthetized with ether and killed by cervical dislocation) were washed with ice-cold saline and incubated for 15 min at 28°C in Ca^{2+}-free saline containing 1 mg/ml collagenase type I (Sigma Chemical Co., St. Louis, MO) plus 0.4 mg/ml DNAse type I (Sigma Chemical Co.), pH 7.3. Washed seminiferous tubules were then incubated for 10 min in Ca^{2+}-free saline containing 0.4 mg/ml trypsin (Worthington Biochemical Corp, Freehold, NJ). Thereafter, tubules were washed twice with Ca^{2+}-free solution supplemented with 1% bovine serum albumin and mechanically dissociated. The resulting cell suspension was stored at 4°C. An aliquot of this suspension was seeded into a Plexiglas recording chamber (RC-25; Warner Instruments, Hamden, CT) placed on the stage of an inverted microscope equipped with phase contrast optics (Nikon Diaphot TMD; Nikon Corp., Tokyo, Japan). The cells remained undisturbed until they attached to the bottom of the recording chamber formed by a No. 1 glass coverslip previously coated with either poly-L-lysine (Sigma Chemical Co.) or Cell-Tack (Collaborative Biomedical Products, Bedford, MA). In early experiments, the pH of the Ca^{2+}-free saline used for dissociation was adjusted to 7.3. However, we noticed that responses to internal alkalinization were more vigorous if the cells had been previously exposed to a slightly more alkaline solution. Thus, all cells used in this study were routinely dissociated and maintained at pH 7.7. Throughout the experiments, cells were superfused with saline whose pH was adjusted to 7.3. All experiments were carried out at room temperature.

Cell Identification

Cells obtained by dissociation of seminiferous tubules from adult testes belong to the most advanced stages of spermatogenesis.

[1]*Abbreviations used in this paper:* AR, acrosome reaction; I-V, current to voltage; SOC, store operated channel.

Spermatocytes, spermatids, and immature sperm are easily recognized under phase contrast by their size and characteristics of nuclei and nucleolus (Bellvé et al., 1977). Pachytene spermatocytes, identified by their condensed nuclear chromatin, are the largest germ cells found in adult testes. Their small size and pale nucleus with a single central nucleolus can recognize round spermatids. Fig. 1 illustrates micrographs, viewed under phase-contrast optics, of freshly dissociated pachytene spermatocytes (*A*), round and condensing spermatids (*B*), condensing spermatid with flagellum (*C*), and testicular sperm (*D*).

Ca^{2+} and pH_i Measurements

Cells were loaded by incubation with the membrane-permeant (AM) form of the Ca^{2+} indicator dye fura-2. In other experiments, the pH-sensitive dye BCECF [(2′,7′)-bis(carboxymethyl)-(5,6)-carboxyfluorescein]-AM was used instead (Molecular Probes, Inc., Eugene, OR). Incubation was initiated by adding to the recording chamber 300 μl of cell suspension and 300 μl of a solution of either 2 μM fura-2 AM or 4 μM BCECF-AM. Cells were allowed to load for 30 (fura-2) or 10 (BCECF) min at room temperature, and then rinsed continuously for another 15 min with recording medium before the beginning of the experiments. Fluorescence of both fura-2 and BCECF appeared diffusely distributed rather than punctate, suggesting that dye compartmentalization was minimal. During the experiments, cells were continuously superfused (~1 ml/min) with recording medium containing (mM): 130 NaCl, 3 KCl, 2 $CaCl_2$, 2 $MgCl_2$, 1 $NaHCO_3$, 0.5 NaH_2PO_4, 5 HEPES, and 5 glucose, pH 7.3.

Intracellular Ca^{2+} levels were determined as previously described (Hernández-Cruz et al., 1997). Briefly, fura-2-loaded cells were imaged with an inverted microscope (Nikon Diaphot TMD), and pairs of images were digitized and recorded using alternating illumination provided by two nitrogen dye lasers tuned at 340 and 380 nm. The pulsed lasers (3-ns pulse duration) were triggered alternately at frequencies ranging from 2 to 15 Hz under computer control. Images at 340 and 380 nm illumination were taken from an area of the coverslip free of cells and stored separately for on-line background subtraction. The key elements of the Ca^{2+} imaging system were a high numerical aperture objective (UV-F 100×, 1.3 NA; Nikon Corp.), an intensified charge coupled device camera (c2400-87; Hamamatsu, Bridgewater, NJ), and the imaging system running under the FL-2 software (Biolase Imaging System, Newton, MA). Ca^{2+} determinations in this study were obtained from individual, entire cells. In the case of sperm, fluorescence measurements were obtained from the head region. Ca^{2+} concentrations were calculated (Grynkiewicz et al., 1985) using the formula $[Ca^{2+}] = K_d\,(F_f/F_b)\,(R - R_{min})/(R_{max} - R)$, where the K_d of fura-2 for Ca^{2+} is 250 nM, F_f/F_b is the ratio of fluorescence values for Ca^{2+}-free/Ca^{2+}-bound indicator at 380 nm excitation, R is the ratio of fluorescence at 340/380 nm for the unknown $[Ca^{2+}]$, and R_{min} and R_{max} are the ratio of fura-2 fluorescence at 340/380 nm of Ca^{2+}-free and Ca^{2+}-bound fura-2. The values of F_f/F_b, R_{min}, and R_{max} for Ca^{2+} were determined by measuring the fluorescence of a glass capillary 100 μm in external diameter containing calibration solutions with 50 μM fura-2 (pentapotassium salt; Molecular Probes, Inc.) and known Ca^{2+} concentrations in the range 10 nM to 40 μM. Although in situ calibrations were attempted, we found it very difficult to manipulate $[Ca^{2+}]_i$ over the required range. Our Ca^{2+} measurements, based only in the in vitro calibrations, could be underestimated to some extent because of effects of viscosity and dye binding to cytoplasmic constituents (Konishi et al., 1988). By comparing fluorescence levels attained 10 min after breaking-in with patch pipettes filled with known concentrations of fura-2 pentapotassium, we estimated that fura-2 reached intracellular concentrations between 20 and 50 μM in the AM-loaded cells.

Intracellular pH measurements were conducted either by single or dual wavelength excitation. In the first case, one of the nitrogen lasers was dye-tuned at 505 nm to illuminate BCECF-

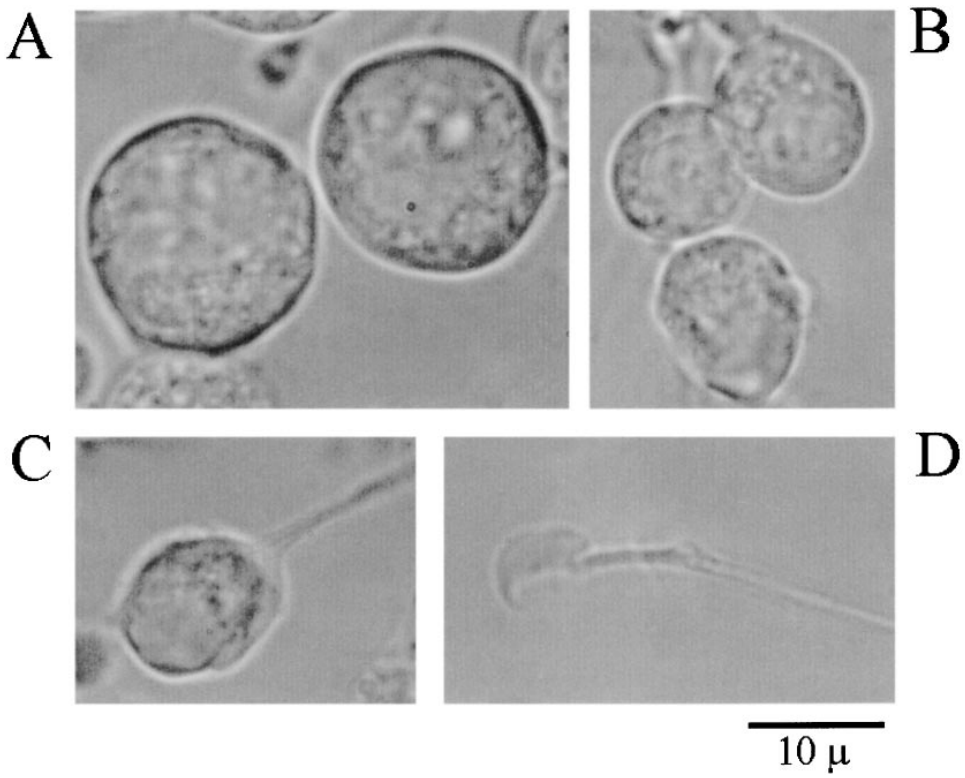

FIGURE 1. Phase contrast micrographs of acutely dissociated spermatogenic cells from adult mouse testis. (*A*) Pachytene spermatocytes, (*B*) round and condensing spermatids, (*C*) immature sperm with flagellum, (*D*) testicular sperm.

loaded spermatogenic cells. Emission light was collected at 520 nm by placing a 510-nm/520-nm dichroic/barrier cube into the microscope light pathway. In these experiments, intended for assessment of pH_i changes with high temporal resolution (<1 s), signals were plotted as differential changes in BCECF fluorescence regarding resting fluorescence ($\Delta F/F_o$). For quantitative pH_i determinations, a different fluorescence imaging system was used. Dual wavelength excitation at 440 and 500 nm was achieved by directing the output of an SLM 8000 spectrofluorometer (SLM Aminco, Rochester, NY) via a fiber optic cable into a B-2A Nikon cube (with the excitation filter removed), placed into the light pathway of an inverted microscope (emission wavelength 520 ± 10 nm). A field containing dye-loaded cells was imaged with a UV objective (UV-F 100×, 1.3 NA) and an intensified charge coupled device camera (c2400-87). Wavelength generation by the spectrofluorometer, as well as image acquisition and fluorescence determination from selected areas of interest, were controlled with the program package Image-1/FL (Universal Imaging Corp., West Chester, PA) running on a PC/AT 66 MHz computer. This system allows continuous ratio measurements of background-corrected BCECF fluorescence at 500/440-nm excitation at intervals of ~2 s. At the end of the experiment, a group of cells was imaged and their 500/440-nm fluorescence monitored during the application of 10 μM of the K^+/H^+ ionophore nigericin in a K^+-rich medium (130 mM KCl, 10 mM NaCl, 1 mM $CaCl_2$, 1 mM $MgCl_2$, 10 mM K-HEPES). This protocol sets pH_i equal to pH_o and was used for in situ calibration of BCECF signals. Fluorescence ratios at 500/440-nm excitation were obtained while the cells were bathed with nigericin-containing external solutions with their pH adjusted with KOH in the range 6.2–9. These ratios were then plotted and the resulting graph was fitted to the Henderson-Hasselbach equation: $pH = pK' + \log (R - R_{min}/R_{max} - R)$. The resulting values for R_{max} and R_{min} (minimum and maximum 500/400-nm ratios), and pK′ were introduced in the same equation to compute pH values from the fluorescence ratios R obtained during the experiments.

Intracellular Alkalinization Procedure

The application of the weak base NH_3 was used to passively alkaliload spermatogenic cells. The solution used contained 25 mM NH_4Cl (osmolarity was maintained with appropriate changes in the amount of NaCl). The pH of the perfusate remained at 7.3. In solution, NH_3 is in chemical equilibrium with its conjugate weak acid, NH_4^+, according to the formula: $NH_3 + H^+ \Leftrightarrow NH_4^+$. When the cells are exposed to the NH_3–NH_4^+ solution, the NH_3 freely crosses the cell membrane and associates with a proton to form NH_4^+. The resulting decrease in free proton concentration causes an increase in pH_i, which continues until $[NH_3]_i$ equals $[NH_3]_o$. The magnitude and rate of rise of the pH_i increase with this method depends on the buffering power of the cell, its initial pH_i, $[NH_3]_o$ in the alkalinization solution, and the membrane permeability to NH_4^+, which tends to acidify the cell. For comparison, experiments were conducted using 25 mM of the permeable weak base trimethylamine instead of NH_4Cl. Similar results were obtained using both methods.

Both the NH_3–NH_4 solution and other test solutions were pressure-applied (10 psi) to the cells by way of puffer pipettes positioned within 100 μm with the aid of manipulators. The solenoid valves of separate Picospritzer II devices (General Valve, Fairfield, NJ) controlled solution application. Control experiments showed that with this procedure, the extracellular medium surrounding the cell was replaced within ~100 ms. Drugs used for different purposes during these experiments were 10 mM caffeine, 10 μM thapsigargin, 50 μM cyclopiazonic acid, 1 μM ionomycin, 30 μM ouabain (Sigma Chemical Co.), 5 μM ryanodine, 20 μM monensin (Calbiochem Corp., San Diego, CA), 10 μM 2-4 dichlorobenzamil (Molecular Probes, Inc.), 5–20 μM nifedipine (Alomone, Jerusalem, Israel), 1 mM $NiCl_2$, 0.5 mM $CdCl_2$, 2 mM $BaCl_2$, 1 mM $MnCl_2$, and 2 mM $SrCl_2$. For experiments requiring Ca^{2+}-free conditions in the external solution, $CaCl_2$ was omitted and the calcium chelator EGTA (0.5 mM) was added.

Electrophysiology

Whole-cell Ca^{2+} currents were recorded using the patch-clamp technique. The recording medium contained (mM): 130 NaCl, 3 KCl, 2 $MgCl_2$, 1 $NaHCO_3$, 0.5 NaH_2PO_4, 5 Na-HEPES, 5 glucose, 10 $CaCl_2$, pH 7.3. The composition of the pipette internal solution was (mM): 110 CsMe, 10 CsF, 15 CsCl, 2 Cs-BAPTA, 4 ATP-Mg, 10 mM phosphocreatine, 5 Cs-HEPES. The pH was adjusted in the range 6.5–8.1 with CsOH. The small liquid junction potential between these solutions (<5 mV; pipette potential negative against bath) was not corrected in this study. Internal Cs^+ was sufficient to block the majority of the small outward K^+ current expressed by these cells. Open-tip pipettes had resistances ranging between 2 and 5 Mohms when filled with pipette solution. Records were filtered (four-pole Bessel filter, bandpass 2 kHz), digitized, and stored. Pulse generation, data acquisition, and analysis were done with a PC computer governed by the pClamp program suite (Axon Instruments, Foster City, CA). Pipette capacitive currents were compensated before rupturing the patch. Once in the whole cell configuration, a holding potential of −80 mV was established, series resistance was electronically compensated, and currents elicited by brief 20-mV depolarizing pulses were averaged. These records were used to determine cell capacitance by digital integration of capacitive transients. Only cells exhibiting adequate voltage control were included in the analysis. Protocols for current–voltage (I-V) relationship and steady state inactivation were consistently used. A p/4 pulse protocol was routinely used to minimize leak and capacitive currents from the current records.

I_{Ca} activation curves were elaborated by converting peak current values from the I-V relationships to conductances using the equation $g_{Ca} = I_{Cap}/(V_m - E_{Ca})$, where I_{Cap} is the peak Ca^{2+} current, V_m the command pulse potential, and E_{Ca} the apparent reversal potential obtained by linear extrapolation of the current values in the ascending portion of the I-V curve. Conductance values were then normalized and fitted to a Boltzmann relation $g/g_{max} = \{1 + \exp[-(V - Va_{1/2})/k_a]\}^{-1}$, where g is the peak conductance, g_{max} the maximal peak Ca^{2+} conductance, $Va_{1/2}$ the midpoint of the activation curve, and k_a the activation steepness factor. The steady state inactivation curve was obtained by eliciting Ca^{2+} currents with a constant 24-ms test depolarization to −20 mV applied at the end of prepulses to different depolarization levels. The amplitude of these 200-ms prepulses was varied in 5-mV steps from −110 to −35 mV. Intervals of 10 s were allowed between consecutive trials to prevent accumulation of inactivation. Current to voltage curves were constructed by plotting peak currents vs. prepulse potentials, and steady state inactivation curves were obtained by normalizing the current values and fitting the data with a Boltzmann equation $I/I_{max} = \{1 + \exp[(V - Vi_{1/2})/k_i]\}^{-1}$, where I is the peak current, I_{max} is the peak current when the prepulse was −110 mV, V is the prepulse potential, $Vi_{1/2}$ is the half-inactivation value, and k_i is the inactivation steepness parameter.

RESULTS

Controlled Rises of Intracellular pH During the Application of NH_4Cl

To test the speed of local perfusion achieved with the puffer pipette and the efficacy of NH_4Cl for inducing

internal alkalinization of spermatogenic cells, single wavelength (505-nm excitation) fluorescence of BCECF-loaded cells was measured during the application of external solution containing 25 mM NH_4Cl. Fig. 2 *A* illustrates the effects of superfusing with NH_4Cl-containing solution a group of four BCECF-loaded spermatogenic cells. Cell alkalinization is indicated by an increase in the ratio $\Delta F/F_o$. pH_i increases rapidly, reaching within 7 s a plateau that remains during the application of NH_4Cl. Upon washout of NH_4Cl, pH_i returned monotonically to baseline. The decay phases of these records could be fitted to single exponential functions, with time constants of 11.4, 11.8, 9.0, and 9.9 s.

Dual wavelength determinations of BCECF signals showed that resting pH_i in spermatogenic cells varies over the range 6.0–7.2. These values are similar to those reported from ram and pig sperm (6.3–6.7; Babcock and Pfeiffer, 1987; Tajima et al., 1987). We did not find consistent pH_i differences among cells from different stages of differentiation (pachytene spermatocytes, 6.74 ± 0.06 [mean ± SEM], n = 18; round and condensed spermatids, 6.63 ± 0.04, n = 44). The application of 25 mM NH_4Cl increased pH_i by 1.35 ± 0.11 pH units, n = 13. This pH_i rise was dependent on the concentration of NH_4Cl (e.g., 5 mM = 0.85 ± 0.04; 15 mM = 1.06 ± 0.06). In contrast to many somatic cells, which exhibit an acidification shift after reaching a peak alkalinization, and a rebound acidification after the removal of NH_4Cl, spermatogenic cells rarely showed any acidification with the pulse duration used in these experiments (see Fig. 2 *A*). This suggests that their plasma membrane lacks an appreciable permeability to NH_4^+ (Bevensee and Boron, 1995). Since the time course of intracellular alkalinization by NH_4Cl can be approximated to a sustained plateau with rapid onset and offset, a correlation between changes of $[Ca^{2+}]_i$ and pH_i changes is possible, making unnecessary the technically more demanding simultaneous measurement of $[Ca^{2+}]_i$ and pH_i (Martínez-Zaguilán et al., 1991, 1996; Wiegmann et al., 1993). Control experiments showed that the time course and amplitude of NH_4Cl-induced alkalinization recorded with BCECF were not greatly affected if the cells had been previously incubated in the presence of fura-2 AM (data not shown).

Alkalinization-induced Changes of Intracellular Ca^{2+} Concentration

In contrast to resting pH_i values, $[Ca^{2+}]_i$ at rest varied significantly among the population of spermatogenic cells: higher resting $[Ca^{2+}]_i$ was consistently determined in cells from more advanced stages of maturation. Thus, pachytene spermatocytes had a mean resting $[Ca^{2+}]_i$ of 56.5 ± 7.2 nM (n = 10), round sperma-

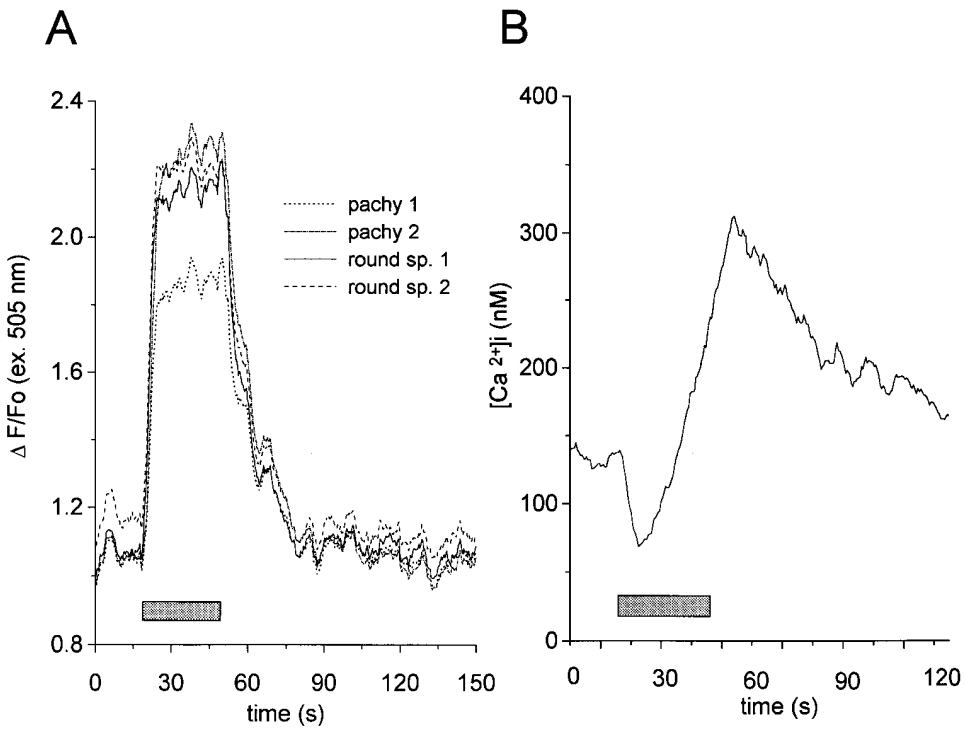

FIGURE 2. (*A*) Time course of intracellular alkalinization induced by NH_4Cl application in two pachytene spermatocytes and two round spermatids. Cells were loaded by incubation with 10 μM BCECF-AM for 20 min. Intracellular pH was monitored as changes of BCECF fluorescence emission (see MATERIALS AND METHODS). The horizontal bar indicates the duration of NH_4Cl application. The internal pH of all cells increases rapidly upon exposure to NH_4Cl, reaching a plateau. Upon removal of the NH_4Cl, intracellular pH returns monotonically to resting levels without a rebound acidification. (*B*) Biphasic changes of intracellular calcium concentration induced by intracellular alkalinization in a fura-2-loaded pachytene spermatocyte. A NH_4Cl-containing puffer pipette placed nearby was used for the controlled intracellular alkalinization. One or more separate pipettes were used for the application of additional test solutions. The horizontal bar represents the duration of NH_4Cl application.

tids of 122.2 ± 13.8 nM (n = 19), and condensing spermatids of 200.2 ± 46.3 nM (n = 5). These differences ($P < 0.02$) are likely to be related to differentiation and maturation of male germ cells. Resting $[Ca^{2+}]_i$ remained stable over periods of observation up to 30 min, suggesting the absence of spontaneous net Ca^{2+} fluxes under our recording conditions.

Alkalinization of spermatogenic cells was generally associated with a characteristic biphasic response composed of an initial $[Ca^{2+}]_i$ drop followed by a delayed rise. An example, recorded from a pachytene spermatocyte is shown in Fig. 2 *B*. Similar changes in $[Ca^{2+}]_i$ were produced by application of the membrane permeant base trimethylamine (25 mM; data not shown). As illustrated in Fig. 3, the initial $[Ca^{2+}]_i$ drop is more apparent in pachytene spermatocytes (*A*) than in round (*B*) or condensing (*C*) spermatids. The opposite is true for the delayed $[Ca^{2+}]_i$ rise. Fig. 3 also shows the progressive increase in the magnitude of the delayed Ca^{2+} rise frequently observed in spermatogenic cells upon repeated applications of NH_4Cl (see below). Although the variability of this facilitation makes the quantitative comparison of responses to different NH_4Cl concentrations difficult, it was clear that concentrations of 10, 15, and 25 mM NH_4Cl produced progressively larger intracellular Ca^{2+} elevations, while 5 mM was ineffective (data not shown). Interestingly, alkalinization with 25 mM NH_4Cl consistently produced similar elevations of $[Ca^{2+}]_i$ in the head region of testicular sperm. An example of these recordings is illustrated in Fig. 4. Some of the testicular sperm examined were immature (they exhibited a cytoplasmic bulge in the middle piece of the flagellum and limited motility; Fig. 4, *inset*), but others were virtually indistinguishable from mature, epididymal sperm. Alkalinization-induced large Ca^{2+} rises appear to be specific to spermatogenic cells from adult mice since they were absent in spermatogonia obtained from testes of 1-wk-old mice (only the initial Ca^{2+} drop component of the response was observed), as well as in other cells tested under similar conditions in our laboratory; i.e., rat sympathetic neurons, rat chromaffin, and pituitary cells (data not shown).

It could be argued that $[Ca^{2+}]_i$ changes recorded with fura-2 may constitute an artifact resulting from pH_i effects on fura-2 dissociation constant for Ca^{2+}

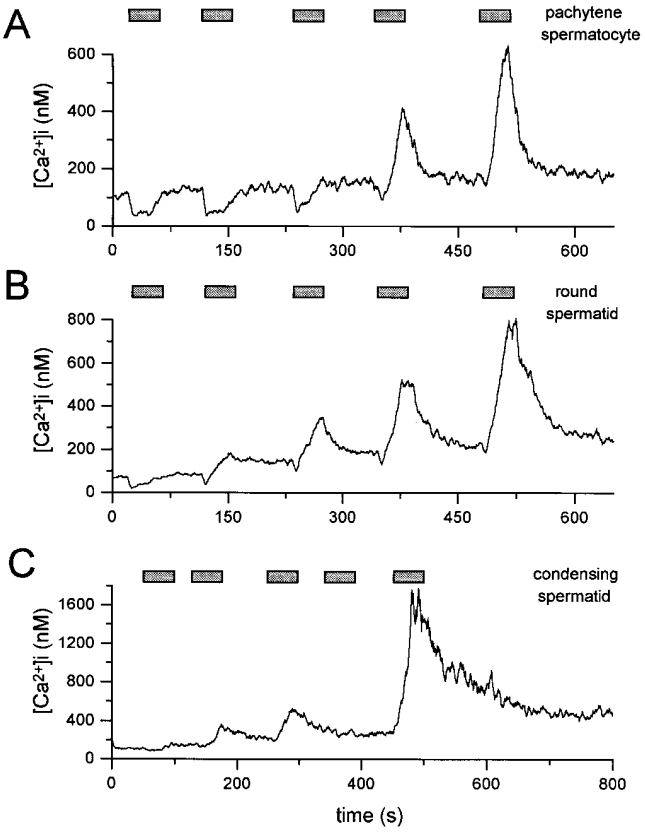

FIGURE 3. Ca^{2+} transients elicited in spermatogenic cells from different stages of maturation after successive applications of NH_4Cl (pulse duration indicated by the horizontal bars). (*A*) Pachytene spermatocyte, (*B*) round spermatid, (*C*) condensing spermatid. Notice that the first application induces an initial $[Ca^{2+}]_i$ drop in the pachytene spermatocyte, which is less noticeable in the round spermatid and virtually absent in the condensing spermatid. Also notice that the magnitude of the Ca^{2+} rise increases with repeated applications of NH_4Cl.

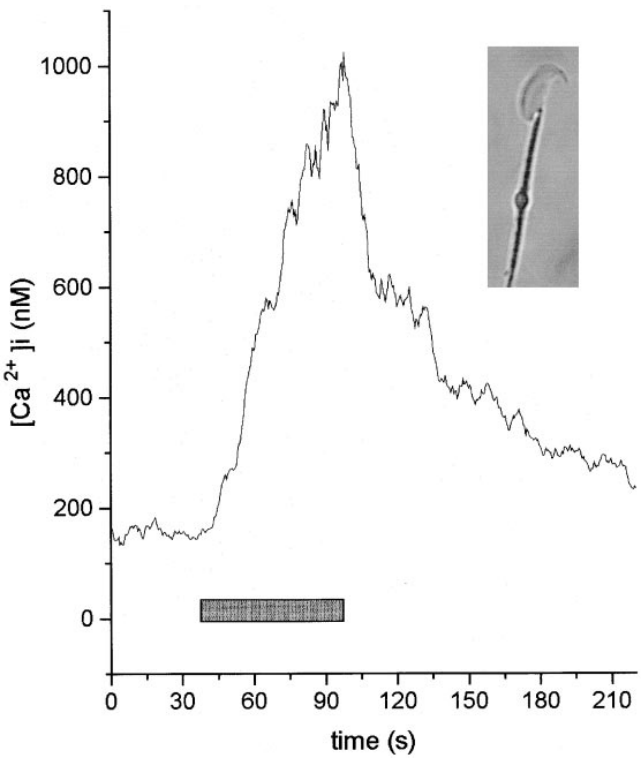

FIGURE 4. $[Ca^{2+}]_i$ transients recorded from the head region of a testicular sperm similar to the one illustrated in the inset. The horizontal bar represents the duration of NH_4Cl application. This response was obtained after the first application of NH_4Cl.

(Martínez-Zaguilán et al., 1991). However, this does not seem likely since most Ca^{2+} measurements of this study were performed at pH_i values where fura-2 properties are pH independent (Batlle et al., 1993; Nitschke et al., 1996). Moreover, experimental maneuvers that modified or even abolished the pH_i-induced Ca^{2+} transients (i.e., experiments done in the absence of external Ca^{2+}; see Fig. 8 *A*) rule out a significant influence of pH on the binding properties of fura-2. Additional considerations emerge from comparisons of the kinetics of the responses. The half-rise time of Ca^{2+} transients among the population of spermatogenic cells ranged from 9.9 ± 1.7 s (pachytene spermatocytes, $n = 4$) to 15.3 ± 2.9 s (condensing spermatids, $n = 4$). In contrast, half-rise times of pH_i signals were faster, ranging from 2.4 ± 0.2 s (round spermatids, $n = 5$) and 2.9 ± 0.2 s (pachytene spermatocytes, $n = 6$) to 4.5 ± 0.4 s (condensing spermatids, $n = 2$). Also, the time constant of decay of $[Ca^{2+}]_i$ signals in pachytene spermatocytes was 12.9 ± 2.9 s ($n = 4$), while the time constant of decay of pH_i signal was 9.9 ± 0.9 s ($n = 5$). In Fig. 5, representative traces of $[Ca^{2+}]_i$ and pH_i from two pachytene spermatocytes are superimposed for comparison. Since effects of internal alkalinization on fura-2 dissociation constant should be immediate, the kinetic differences between $[Ca^{2+}]_i$ and pH_i responses suggest that the $[Ca^{2+}]_i$ rise constitutes a genuine physiological response.

Since alkalinization-induced Ca^{2+} rises are bigger and faster in condensing and round spermatids than in pachytene spermatocytes, we hypothesized that perhaps the rise was concealing the initial drop. Experiments shown in Figs. 3 and 6 appear to support this explanation. Fig. 6 *A*, obtained from a pachytene spermatocyte, shows the increasing magnitude of alkalinization-induced Ca^{2+} rises with repeated NH_4Cl applications. The four successive responses shown in Fig. 6 *A* were aligned and superimposed in Fig. 6 *B* for comparison. As these $[Ca^{2+}]_i$ records clearly show, the use-dependent facilitation of the Ca^{2+} rise determines the gradual obliteration of the initial Ca^{2+} drop. Also, notice that the magnitude of the initial Ca^{2+} drop does not facilitate as the Ca^{2+} rise does.

Alkalinization-induced Early Ca^{2+} Drop

The initial $[Ca^{2+}]_i$ drop, which is most clearly observed in pachytene spermatocytes, (*a*) develops without apparent delay regarding the pH_i increase, (*b*) does not exhibit facilitation, and (*c*) lasts for as long as the NH_4Cl application is maintained when the delayed rise is absent or has been eliminated (see Figs. 3 *A*, 7 *B*, and 8 *A*). These characteristics suggest that the initial Ca^{2+} drop has a different mechanism than the delayed Ca^{2+} rise. Several hypotheses can be offered to explain the initial Ca^{2+} drop. We favor the most parsimonious one; that is, upon entering the cell, NH_3 displaces H^+ from Ca^{2+} binding sites on proteins, increasing the buffering power of the cell and hence diminishing resting $[Ca^{2+}]_i$. Further experiments are being planned to determine the precise nature of the initial Ca^{2+} drop. The remainder of this paper will focus on the nature of the delayed $[Ca^{2+}]_i$ rise.

Use-dependent Facilitation of the $[Ca^{2+}]_i$ Rise

In early experiments, we noticed that preincubation of the cells in a slightly more alkaline medium promoted the appearance of $[Ca^{2+}]_i$ rises. Thus, cells incubated at external pH 7.7 had a $pH_i = 6.6 \pm 0.03$ ($n = 62$) and

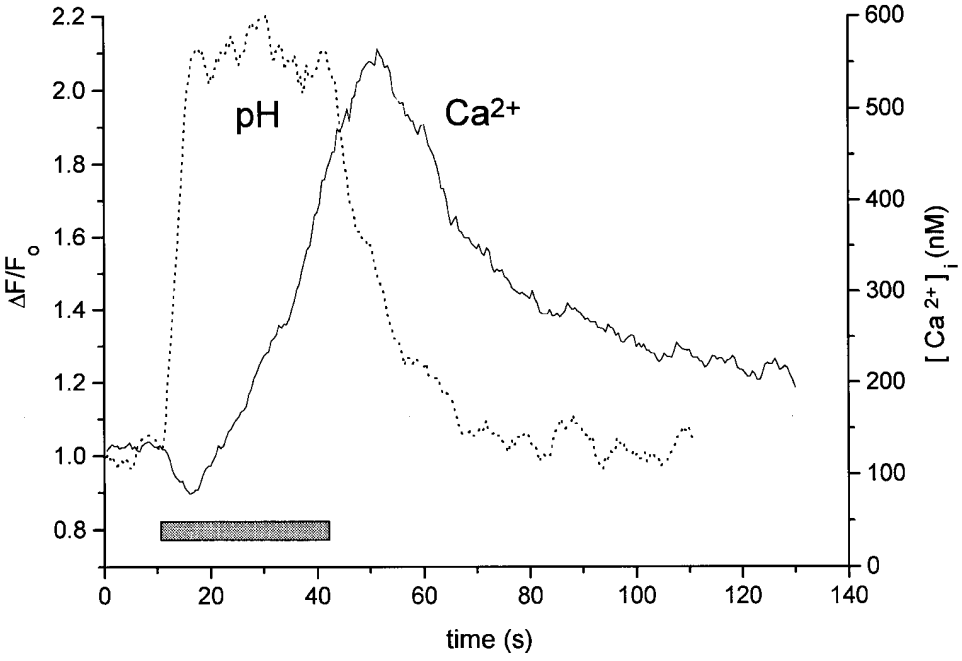

FIGURE 5. Representative recordings of $[Ca^{2+}]_i$ and pH_i obtained from two different pachytene spermatocytes loaded with BCECF and fura-2, respectively. Traces were superimposed for comparison. Notice that the initial $[Ca^{2+}]_i$ drop occurs almost simultaneously with the pH_i rise elicited by NH_4Cl application (*horizontal bar*), while the $[Ca^{2+}]_i$ elevation appears with a significant delay.

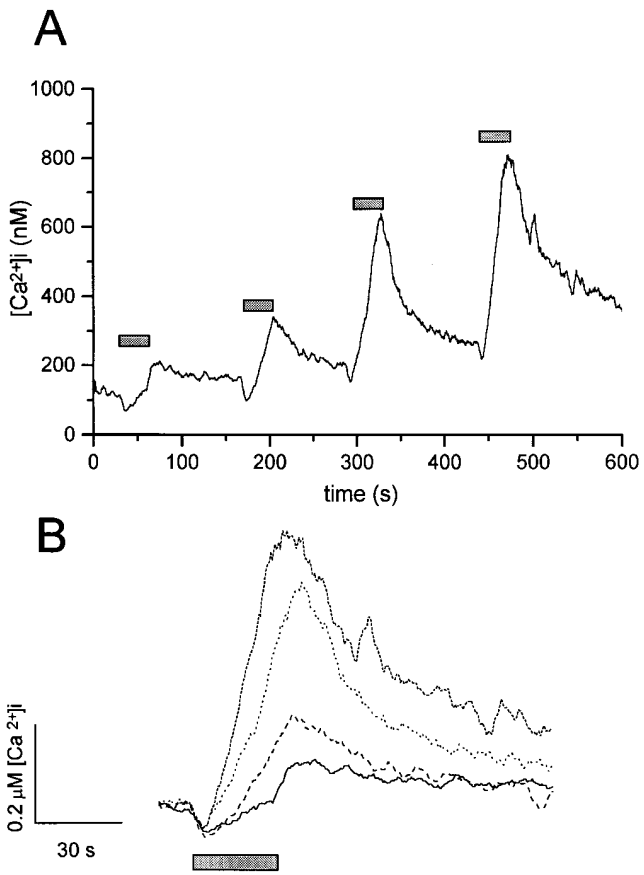

FIGURE 6. Facilitation of $[Ca^{2+}]_i$ transients. (*A*) $[Ca^{2+}]_i$ rises recorded from a pachytene spermatocyte show use-dependent facilitation upon repeated application of NH_4Cl (*horizontal bars*). Notice that both the magnitude and the rate of rise of $[Ca^{2+}]_i$ transients became larger. Conversely, $[Ca^{2+}]_i$ transients decay more slowly after repeated intracellular alkalinizations. (*B*) Superimposed responses to the NH_4Cl applications shown in *A*. Traces were aligned both vertically and horizontally for clarity. Notice that the magnitude of the initial $[Ca^{2+}]_i$ drop remains invariant, becoming progressively obliterated by the delayed $[Ca^{2+}]_i$ rise.

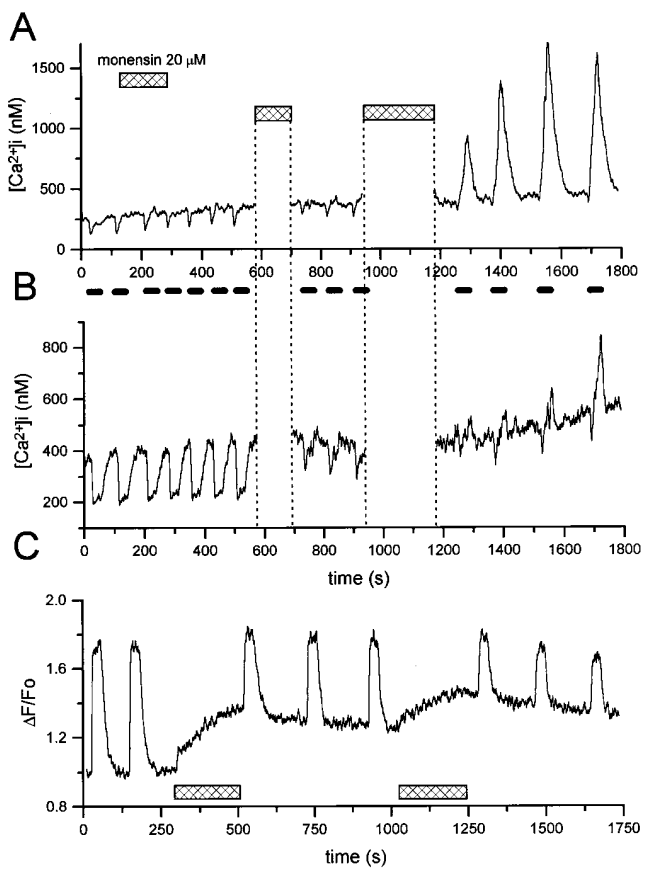

FIGURE 7. Development of $[Ca^{2+}]_i$ responses after incubation with monensin. (*A* and *B*) Recordings obtained from two fura-2-loaded spermatogenic cells that initially failed to show a $[Ca^{2+}]_i$ rise component upon stimulation with NH_4Cl (pulses indicated with the filled horizontal bars). After 2-min incubation with 20 μM monensin, cells began to respond with small Ca^{2+} rises. These responses increased after a second monensin incubation for 4 min. Monensin-treated cells showed both Ca^{2+} rises and use-dependent facilitation of the responses. (*C*) Recording of fluorescence changes in a BCECF-loaded spermatogenic cell. The experiment was designed to determine if use-dependent facilitation results from a progressive increase in resting pH_i. The first part of the record shows that pH_i returns completely to resting levels between successive NH_4Cl applications. The second part of the record shows that after monensin application, basal pH_i rises without increasing the magnitude of the pH_i rise elicited by NH_4Cl application. Also notice that responses to NH_4Cl after monensin incubation decay completely to prestimulation levels.

quite often responded with $[Ca^{2+}]_i$ rises to the application of 25 mM NH_4Cl, while cells kept at pH 7.3 were significantly more acidic (6.4 ± 0.03, $n = 100$, $P = 2.1 \times 10^{-8}$) and responded less frequently with increases in $[Ca^{2+}]_i$ (only the initial Ca^{2+} drop was observed). Therefore, we speculated that the appearance of alkalinization-induced $[Ca^{2+}]_i$ rises could be more likely to occur when pH_i reaches a critical value. Support for this "pH_i threshold hypothesis" comes from experiments such as the one illustrated in Fig. 7, *A* and *B*. Here, two initially unresponsive cells (notice the lack of $[Ca^{2+}]_i$ rises upon repeated pulsing with NH_4Cl), were incubated for 2 min in the presence of 20 μM monensin, a Na^+ ionophore that exchanges external Na^+ for internal H^+, thus alkalinizing the cytoplasm. Shortly after incubation in the presence of monensin, the cells began to respond with small Ca^{2+} rises to the application of NH_4Cl. Moreover, after a second monensin application for 4 min, cells showed both Ca^{2+} rise and use-dependent facilitation of the responses. In separate experiments, we noticed that the pH_i of BCECF-loaded cells climbed from 6.57 ± 0.17 to 6.89 ± 0.20 ($n = 3$) after 4 min of monensin application. These data suggest that cells begin to show $[Ca^{2+}]_i$ rises in response to alkalinization when resting pH_i exceeds ~6.7. As explained later, this finding may be relevant for the sperm capacitation process.

As previously shown, spermatogenic cells display facilitation of the Ca^{2+} rise upon repeated applications of

NH_4Cl. Sometimes this phenomenon is accompanied by a sustained increase in resting $[Ca^{2+}]_i$, but not necessarily. In fact, normal facilitation is observed in cells that had been pulsed with NH_4Cl in Ca^{2+}-free medium, thus preventing Ca^{2+} influx (data not shown). The question that immediately rises is, does use-dependent facilitation also result from a progressive, sustained increase in resting pH_i? The experiment shown in Fig. 7 *C* was designed to test this hypothesis. As shown in the first part of the record (initial two responses), the pH_i returns completely to resting levels between successive NH_4Cl pulses. Control experiments showed that both the sizes of pH_i deflections and the resting pH_i remained unchanged during repetitive NH_4Cl applications (data not shown). The second part illustrates the effects of monensin application. Clearly, monensin raises basal pH_i without increasing the magnitude of the pH_i change resulting from each NH_4Cl application. Also, the response to NH_4Cl in the presence of monensin decays completely to prestimulation levels. Similar results were obtained in five additional cells. These findings rule out an incremental rise of resting pH_i as an explanation to the use-dependent facilitation phenomenon. More likely, a pH-dependent regulatory mechanism capable of inducing long term modifications of the permeation pathway either directly or by way of second messengers (e.g., cyclic AMP; Trimmer and Vacquier, 1986; Gabers, 1989; Beltrán et al., 1996; Arnoult et al., 1997) underlies the use-dependent facilitation of the Ca^{2+} rise. These and other possible explanations to the facilitation phenomenon are yet to be explored.

Source of Ca^{2+} Underlying the $[Ca^{2+}]_i$ Rise

The $[Ca^{2+}]_i$ elevation secondary to internal alkalinization could result from plasmalemmal Ca^{2+} influx, intracellular Ca^{2+} release, or both. Experiments such as those exemplified in Fig. 8 explored the possible contribution of external Ca^{2+}. Here, two puffer pipettes were positioned near the cell and the recording chamber was continuously bathed with Ca^{2+}-free external solution when indicated. Both pipettes contained NH_4Cl, but only one of them contained 2 mM $CaCl_2$. As shown in Fig. 8 *A*, the application of NH_4Cl in the complete absence of external Ca^{2+} resulted only in the appearance of the $[Ca^{2+}]_i$ drop. When the pulse of NH_4Cl was delivered through the pipette containing 2 mM Ca^{2+}, the $[Ca^{2+}]_i$ rise reappeared, masking the initial drop. In this case, as in most spermatocytes examined, Ca^{2+} influx is clearly required for the alkalinization-induced $[Ca^{2+}]_i$ rise. This result may have two possible explanations: either Ca^{2+} influx is the sole source of the Ca^{2+} transient or a combination of influx and release (that is, through the process termed Ca^{2+}-induced Ca^{2+} release) is involved. Fig. 8 *B* illustrates the result of a similar experiment in a condensing spermatid. The main difference here is that in spite of the absence of external Ca^{2+}, alkalinization can still produce a small $[Ca^{2+}]_i$ rise. The source of this $[Ca^{2+}]_i$ rise remains to be identified, although an intracellular Ca^{2+} source is the most likely explanation. It should be pointed out that responses such as those illustrated in Fig. 8 *B* were observed in the minority (~10%) of all spermatids examined.

To directly assess the availability of releasable Ca^{2+} from intracellular stores, we tested the effects of caffeine and ryanodine (10 mM and 5 μM, respectively). These plant alkaloids are agonist and antagonist, respectively, of ryanodine receptor/Ca^{2+} release channels. As shown in Fig. 9, *A* and *B*, neither caffeine nor ryanodine per se induced a significant Ca^{2+} rise in spermatogenic cells. We also tested the effects of thapsigargin and cyclopiazonic acid, specific inhibitors of the Ca^{2+}-ATPase of the

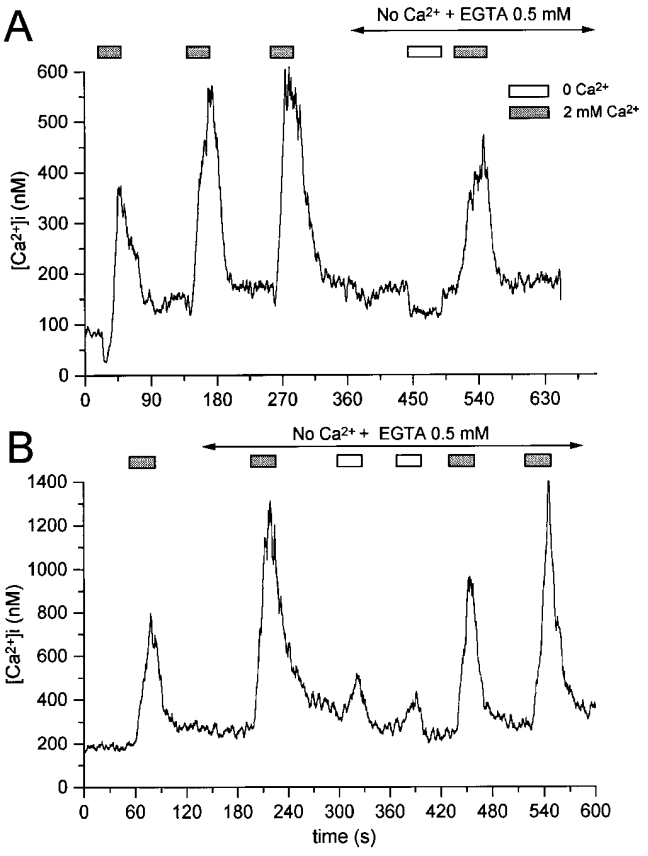

FIGURE 8. Contribution of external Ca^{2+} to the alkalinization-induced $[Ca^{2+}]_i$ transients in spermatogenic cells. Ca^{2+} rises were recorded first in normal recording solution, and then in a solution containing no added Ca^{2+} and 0.5 mM EGTA. Along with the standard puffer pipette, a second pipette containing NH_4Cl and no Ca^{2+} was used to induce intracellular alkalinization while keeping Ca^{2+}-free conditions. Responses were obtained from a pachytene spermatocyte (*A*) and a condensing spermatid (*B*). Notice that when NH_4Cl is applied in the complete absence of external Ca^{2+}, the delayed Ca^{2+} rise is either suppressed (*A*) or greatly reduced (*B*). Also, notice in *A* that the initial Ca^{2+} drop obliterated by the delayed Ca^{2+} rise becomes discernible upon removal of extracellular Ca^{2+}.

endoplasmic reticulum (10 and 50 μM, respectively). As shown in Fig. 9, *C* and *D*, when these drugs were applied, they produced either no effect or a modest Ca^{2+} release. Interestingly, these inhibitors only elicited noticeable Ca^{2+} rises in cells from less advanced stages of differentiation (e.g., pachytene spermatocytes). When internal alkalinization was induced after the application of these drugs (the effects of some of which are considered irreversible), Ca^{2+} signals of normal appearance were elicited (see Fig. 9, *A–C*). As shown in Fig. 9 *E*, even the application of 1 μM ionomycin (a divalent cation ionophore used to increase the permeability of biological membranes to Ca^{2+}, which also depletes a variety of intracellular Ca^{2+} stores), without external Ca^{2+}, produced small Ca^{2+} rises in spermatogenic cells. To test the efficacy of ionomycin, the same cells were exposed to the ionophore while bathed in Ca^{2+}-free medium, and then perfused with a solution containing no ionomycin and 2 mM Ca^{2+}. This was rapidly followed by a large Ca^{2+} rise (Fig. 9 *E, middle*). This rise may result from Ca^{2+} influx through ionomycin remaining in the plasma membrane, store-operated

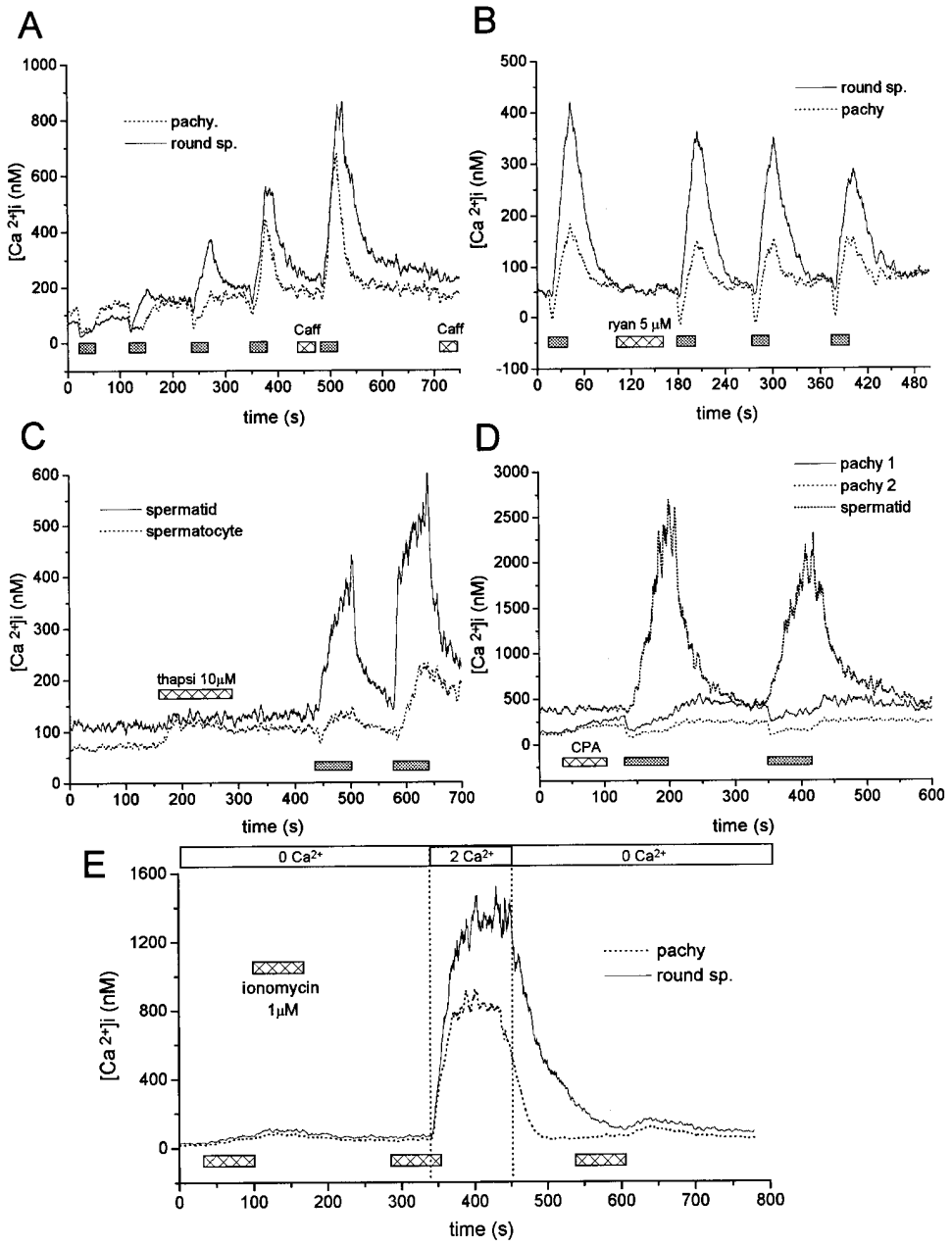

FIGURE 9. Effects of agents affecting Ca^{2+} mobilization from intracellular stores. (*A*) Ca^{2+} recordings obtained from a pachytene spermatocyte and a round spermatid upon repeated applications of NH_4Cl. When indicated, caffeine (10 mM) was applied from a second puffer pipette. Caffeine neither induced Ca^{2+} rises in spermatogenic cells nor affected their responses to subsequent NH_4Cl applications. (*B*) In another cell pair, 5 μM ryanodine was also ineffective as a Ca^{2+} release agent. Although the responses to NH_4Cl diminished slightly after ryanodine exposure, this result was not observed in other cells tested. (*C*) The effects of 10 μM thapsigargin were tested in a round spermatid and a pachytene spermatocyte. The figure is representative of more than 12 cells similarly examined. Notice that only the relatively less differentiated spermatocyte showed a modest Ca^{2+} rise. (*D*) Effects of cyclopiazonic acid (*CPA*) on resting Ca^{2+} levels and responses to alkalinization in three spermatogenic cells. CPA induced small Ca^{2+} rises in both pachytene spermatocytes, but not in the round spermatid. Responses to NH_4Cl after incubation with thapsigargin or CPA appear similar to those of untreated cells. (*E*) Effects of ionomycin. When two spermatogenic cells were exposed to 1 μM ionomycin without external Ca^{2+}, they exhibit small Ca^{2+} rises, suggesting that the Ca^{2+} content of the intracellular reservoirs is low. In contrast, the same stimulus induced a large increase of intracellular Ca^{2+} when external medium was switched to one containing normal external [Ca^{2+}]. This elevation is likely due to plasmalemmal Ca^{2+} influx through ionomycin pores. Reapplication of ionomycin without external Ca^{2+} after such a large Ca^{2+} load is still unable to release a substantial amount of Ca^{2+}.

channels activated by depletion during the initial ionomycin application, or both (see below). When ionomycin was applied shortly after this substantial Ca^{2+} load, it was still ineffective to produce a large Ca^{2+} release, suggesting that Ca^{2+} uptake into intracellular stores is negligible within the time scale of this experiment. Taken together, these data suggest that the amount of Ca^{2+} available for release from rapidly exchanging intracellular reservoirs is too small to directly contribute to the Ca^{2+} transient induced by cytosolic alkalinization. Nonetheless, intracellular Ca^{2+} release could contribute indirectly, by activating store-operated channels (SOCs) whose presence has not been examined in spermatogenic cells. An alternative interpretation of the experiment shown in Fig. 9 *E* could be that, after the initial treatment with ionomycin, the stores become depleted, leading to the opening of SOCs. Subsequent addition of external Ca^{2+} would then result in a large Ca^{2+} influx mediated by SOCs rather than by ionomycin remaining in the plasmalemma. In fact, such a protocol (depletion of stores in Ca^{2+}-free medium followed by readmission of external Ca^{2+}) is often used to reveal SOCs (Parekh and Penner, 1997). To explore this possibility, we performed the classical protocol, but using thapsigargin instead of ionomycin. Thapsigargin was chosen because it specifically inhibits intracellular pumps and lacks ionophoric or detergent activity. The result of such an experiment is shown in Fig. 10. Here, a group of eight spermatogenic cells was exposed to thapsigargin (10 μM) for 3 min with the aid of a puffer pipette (Ca^{2+}-free conditions effective for the whole time). A few minutes later, a medium containing 2 mM Ca^{2+} was applied to the cells with a second puffer pipette. This was followed by a slow and sustained Ca^{2+} influx that ceased upon removal of external Ca^{2+}. These results suggested that (*a*) thapsigargin depleted the stores, albeit without an apparent Ca^{2+} rise, and (*b*) spermatogenic cells appear to express SOCs. It remains to be explored whether a pH-induced depletion of Ca^{2+} stores may lead to opening of SOCs and if this permeation pathway can account for the alkalinization-induced Ca^{2+} transient (see DISCUSSION).

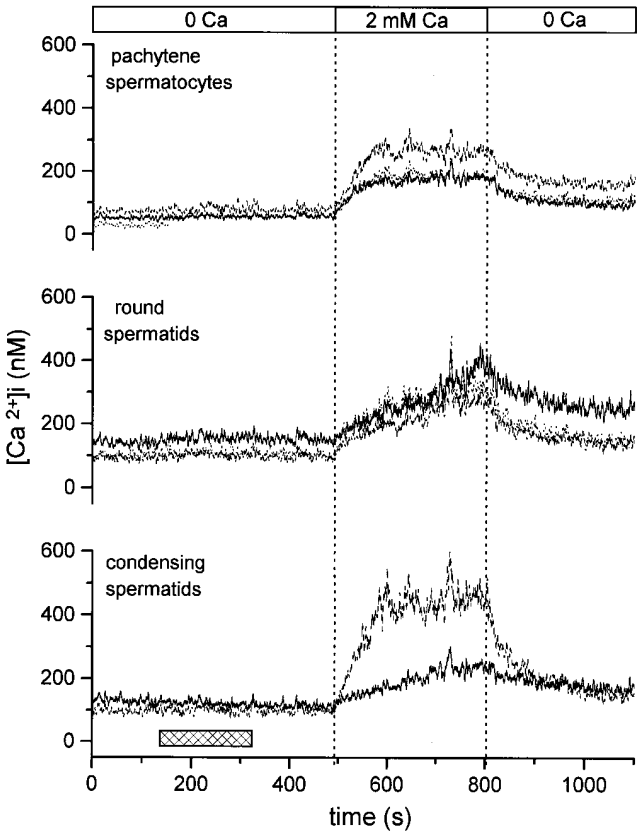

FIGURE 10. Evidence for the presence of store-operated channels in spermatogenic cells. A group of eight spermatogenic cells, continuously bathed in Ca^{2+}-free medium, were transiently exposed to Ca^{2+}-free medium containing 10 μM thapsigargin when indicated (*horizontal bar*). Thapsigargin induced either no response or only a small Ca^{2+} rise, suggesting either that the Ca^{2+} content of the intracellular reservoirs is low or that Ca^{2+} is extruded from the cell as fast as it is released. When the cells were perfused with a puffer pipette filled with medium containing 2 mM Ca^{2+}, an increase of intracellular Ca^{2+} was observed. The same maneuver had no effects on Ca^{2+} levels before the application of thapsigargin (not shown). Ca^{2+} elevation upon exposure to external Ca^{2+} is likely due to plasmalemmal Ca^{2+} influx mediated by store operated channels.

Permeation Properties of the pH-sensitive Ca^{2+} Influx Pathway in Spermatogenic Cells

To examine the selectivity of the Ca^{2+} permeation pathway, the recording chamber was continuously perfused with Ca^{2+}-free external solution, and either Sr^{2+} or Ba^{2+} substituted Ca^{2+} in the NH_4Cl-containing puffer pipette. This protocol was used to warrant that the cells were only exposed to the test divalent cation during the episode of intracellular alkalinization. Fig. 11, *A* and *B,* shows results obtained from two round spermatids. Here, fluorescence ratios of 340/380 nm were plotted rather than intracellular concentrations of divalent cations because fura-2 dissociation constants for Sr^{2+} and Ba^{2+} differ considerably from that of Ca^{2+}. Although these experiments only provide semi-quantitative information of divalent plasmalemmal fluxes, they clearly demonstrate that Ca^{2+}, and to a large extent Sr^{2+} and Ba^{2+}, can permeate through the influx pathway made available by intracellular alkalinization.

To further examine the permeation characteristics of the Ca^{2+} influx pathway, cells were bathed with Ca^{2+}-free saline, and then exposed to the NH_4Cl-containing solution, first in the absence, and then in the presence of 1 mM Mn^{2+}. Here, fura-2 fluorescence was monitored at 340-nm excitation. At this excitation wavelength, Ca^{2+} or Mn^{2+} influx should lead to opposite signals: Ca^{2+} influx producing a fluorescence increase, and Mn^{2+} entry producing a decrease because of

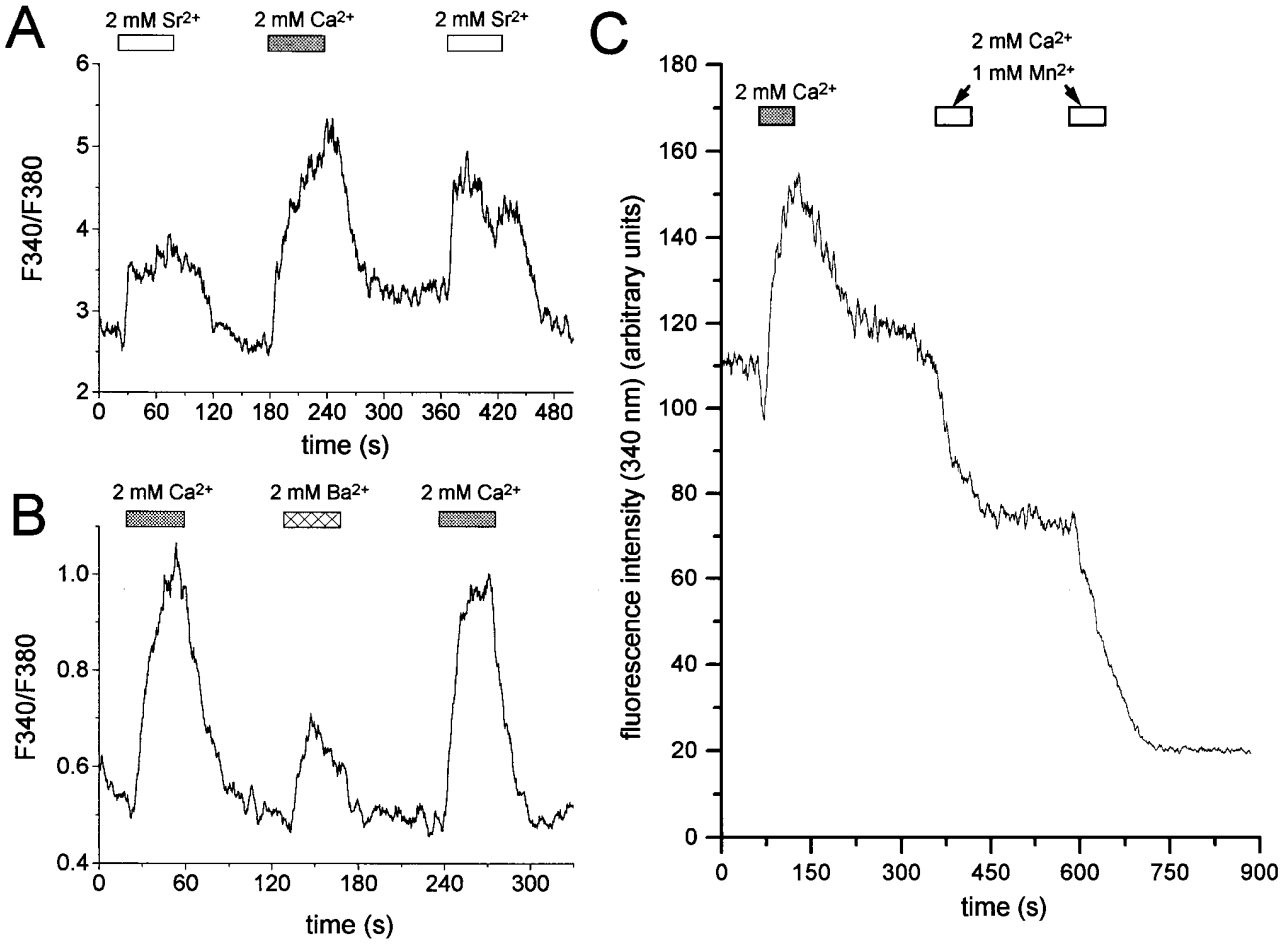

FIGURE 11. Selectivity of the permeation pathway induced by intracellular alkalinization. (*A* and *B*) Experiments were conducted in round spermatids to explore the effects of substituting Sr^{2+} or Ba^{2+} for Ca^{2+} in the NH_4Cl-containing solution. Ca^{2+}-free solution supplemented with 0.5 mM EGTA was continuously superfused to ensure that the cell was exposed only to the test divalent cation during intracellular alkalinization. Only fluorescence ratios 340/380 nm are shown since dissociation constants of fura-2 for Sr^{2+} and Ba^{2+} differ considerably from that of Ca^{2+}. Both Sr^{2+} (*A*) and Ba^{2+} (*B*) can permeate through the Ca^{2+} influx pathway made available by intracellular alkalinization. (*C*) Mn^{2+} permeates the alkalinization-induced Ca^{2+} influx pathway. In this experiment, fluorescence of fura-2 at 340 nm was monitored. At this wavelength Ca^{2+} influx appears as a fluorescence increase, while Mn^{2+} entry appears as a decrease in fluorescence. Application of NH_4Cl in the absence of Mn^{2+} (*filled bar*) induces the characteristic initial drop followed by delayed Ca^{2+} rise. In contrast, a fluorescence decrease is observed when alkalinization is produced with a puffer pipette also containing 1 mM Mn^{2+} (*open bars*). Notice that each application of NH_4Cl in the presence of Mn^{2+} produces a step-like irreversible fluorescence loss, consistent with Mn^{2+} entering the cell and quenching a fraction of fura-2 fluorescence.

quenching of fura-2 emission. As shown in Fig. 11 *C*, the application of NH_4Cl without Mn^{2+} (*filled bar*) induces the characteristic initial $[Ca^{2+}]_i$ drop followed by a delayed increase in $[Ca^{2+}]_i$. In contrast, in the presence of 1 mM Mn^{2+} (*open bars*), alkalinization only produces a decrease in fluorescence. Moreover, a drop in fluorescence emission follows each application of NH_4Cl. This is consistent with Mn^{2+} entering the cell through the permeation pathway regulated by intracellular alkalinization, followed by the irreversible quenching of a fraction of fura-2 by Mn^{2+}. It is noteworthy that fluorescence increases due to Ca^{2+} influx were not observed during internal alkalinization in the presence of Mn^{2+}. One interpretation is that the pH-regulated permeation pathway is exceedingly more permeable to Mn^{2+} than to Ca^{2+}. However, a comparison based on fluorescence changes is inappropriate because fura-2 has a 40-fold higher affinity for Mn^{2+} than for Ca^{2+} (Grynkiewicz et al., 1985), and a small Ca^{2+} influx could be vastly underestimated. Clearly, membrane current measurements would be the correct approach to decide this matter.

Role of Voltage-gated Ca^{2+} Channels in the Alkalinization-induced Ca^{2+} Influx (Effects of Inorganic and Organic Ca^{2+} Channel Blockers)

Recent reports have suggested that T-type Ca^{2+} channels expressed in late spermatogenic cells may contrib-

ute to the Ca^{2+} influx necessary to initiate the sperm acrosome reaction (Arnoult et al., 1996*b*; Liévano et al., 1996; Santi et al., 1996). This notion is supported by earlier observations that Ni^{2+}, dihydropyridines such as PN200-110, and nifedipine (Florman et al., 1992), as well as amiloride and pimozide, which inhibit the acrosome reaction, also block spermatogenic cell Ca^{2+} currents (Arnoult et al., 1996*b*; Liévano et al., 1996; Santi et al., 1996).

To explore whether voltage-gated Ca^{2+} channels contribute to the Ca^{2+} permeation pathway induced by internal alkalinization, we tested the effect of inorganic divalent Ca^{2+} channel blockers Cd^{2+} and Ni^{2+}. Cd^{2+} (0.5 mM) and Ni^{2+} (0.2 and 1 mM) invariably inhibited the delayed Ca^{2+} transient. Ni^{2+} was able to completely block Ca^{2+} rises when they were small, but when the responses became facilitated after repeated NH_4Cl applications, a progressively larger fraction of the Ca^{2+} rise remained unblocked (data not shown). Fig. 12 *A* shows the effects of pulsing with NH_4Cl, a pachytene spermatocyte, both with and without 1 mM Ni^{2+}. This protocol was designed to take into account the facilitatory effect resulting from repeated alkalinization on the magnitude of the Ca^{2+} transients. Alkalinization-induced responses were smaller and rose more slowly in the presence of Ni^{2+}. The effect of Ni^{2+} on the kinetics of Ca^{2+} transients in another pachytene spermatocyte is shown in Fig. 12 *B*. Here, responses to alternate applications of NH_4Cl with and without Ni^{2+} are superimposed for comparison. Upon the application of NH_4Cl plus Ni^{2+}, the delayed Ca^{2+} rise was drastically inhibited, without affecting the kinetics or magnitude of the initial $[Ca^{2+}]_i$ drop. Ni^{2+} inhibited alkalinization-induced Ca^{2+} transients at concentrations as low as 200 μM.

In separate experiments, we tested the effects of nifedipine (an organic blocker effective on the Ca^{2+} channels present in spermatogenic cells; Santi et al., 1996) on the Ca^{2+} transients elicited by internal alkalinization. Fig. 12 *C* illustrates responses of a pachytene spermatocyte to the repeated application of NH_4Cl, first in the absence, and then in the presence of 20 μM nifedipine. Nifedipine did not affect the magnitude of the Ca^{2+} transients or their use-dependent facilitation. Since dihydropyridines are very photolabile, the lack of effect on the alkalinization-induced Ca^{2+} permeation pathway could be due to its destruction by the laser illumination. To rule out this possibility, the last puffer application of NH_4Cl and nifedipine in Fig. 12 *C* was given with the laser illumination omitted. At the end of the NH_4Cl application, the laser illumination was turned on again. It is obvious from this recording that $[Ca^{2+}]_i$ had risen to an even higher level than in the previous NH_4Cl application, suggesting that photolysis of nifedipine is not responsible for the drug's lack of effect. Additional experiments, carried out with 20 μM nifedipine bathing the recording chamber for >10 min be-

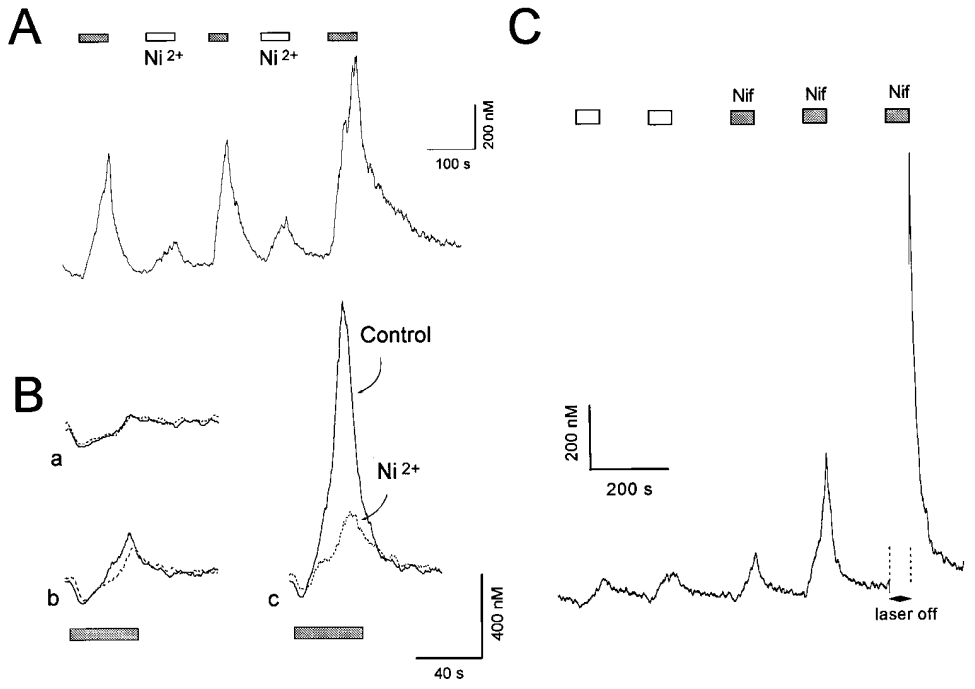

FIGURE 12. Effects of Ni^{2+} and nifedipine on the alkalinization-induced Ca^{2+} entry pathway. (*A*) Ca^{2+} transients recorded from a pachytene spermatocyte upon alternate puffer applications of NH_4Cl both in the absence (*filled bars*) and presence (*open bars*) of 1 mM $NiCl_2$. The bathing external solution contained no Ca^{2+}, while the solution in both pipettes contained 2 mM Ca^{2+}. Alkalinization-induced Ca^{2+} transients were consistently smaller and had a slower rate of rise in the presence of Ni^{2+}. (*B*) Comparison of responses obtained from a different spermatocyte upon alternate intracellular alkalinizations by NH_4Cl applications, both in the absence (*continuous line*) and presence (*dashed line*) of 1 mM Ni^{2+}. *a–c* are consecutive alternate responses. Notice that Ni^{2+} inhibits the delayed Ca^{2+} rise without affecting the initial Ca^{2+} drop. (*C*) Responses obtained from a pachytene spermatocyte to the repeated application of NH_4Cl, first in the absence (*open bars*) and then presence (*filled bars*) of 20 μM nifedipine in the pipette solution. The last puffer application of NH_4Cl and nifedipine was given with the laser illumination turned off to prevent the possible photolysis of the drug.

fore the beginning of the recording, confirmed that nifedipine does not inhibit the Ca^{2+} permeation pathway. These pharmacological results were inconclusive as far as the role of T-type Ca^{2+} channels was concerned, since an effective blocker (Ni^{2+}) inhibited the response to alkalinization, while the other (nifedipine) did not.

Effects of Intracellular Alkalinization on the Properties of T-type Ca^{2+} Currents

It has been pointed out that the fast inactivation of T-type Ca^{2+} channels upon membrane depolarization would prevent them from significantly contributing to the sustained elevation of $[Ca^{2+}]_i$ required for the acrosome reaction (Santi et al., 1996; Arnoult et al., 1996*a*, 1996*b*). Nevertheless, different mechanisms can be postulated by which the activity of T-type Ca^{2+} channels could allow more prolonged Ca^{2+} rises. T-type Ca^{2+} channels could contribute to a sustained Ca^{2+} rise if ZP3-induced intracellular signals, such as the elevation of pH_i (Florman et al., 1989; Florman, 1994) or a change in the phosphorylation state of the channels (Liévano et al., 1996; Arnoult et al., 1997), drastically affect one or more of their biophysical properties (e.g., activation threshold, rate of inactivation, "window current," number of active channels). For instance, a sustained Ca^{2+} influx carried by T-type Ca^{2+} channels could be expected if they become substantially less rapidly inactivating or if the window current (the area under the point of crossing of activation and steady state inactivation curves) increases.

To test directly the possibility that alkalinization affects Ca^{2+} currents, the currents were recorded using pipette internal solutions tailored at two different pH_i values (7.4 and 8.1), as well as external solution at pH 8.1. The results are summarized in Fig. 13 *A*, which illustrates peak Ca^{2+} current densities obtained for these experimental conditions (see Santi et al., 1996). When the intracellular pH was raised from 7.4 to 8.1 (keeping external pH constant), peak Ca^{2+} current density increased significantly (from 7.52 ± 0.41 to 9.06 ± 0.2 $\mu A/cm^2$). A larger increase (to 9.52 ± 0.41 $\mu A/cm^2$) was observed when external pH increased from 7.3 to 8.1 (keeping pH_i constant). Current density measured in cells recorded with an internal solution made to pH 6.5 (close to the cell's measured resting pH_i) was 7.45 ± 0.22 $\mu A/cm^2$, $n = 3$. This value is not different from that obtained at pH_i 7.4. Representative families of Ca^{2+} currents obtained at pH_i 7.4 and 8.1 and pH_o 8.1 are shown in Fig. 13 *B*. Mean I-V relationships obtained from the three experimental groups are shown in Fig. 14 *A*. Rising intracellular pH from 7.4 to 8.1 significantly increased peak Ca^{2+} current density (from 6.31 ± 0.83 to 8.49 ± 0.25 $\mu A/cm^2$). A larger increase (to 9.62 ± 0.61 $\mu A/cm^2$) was observed when external pH increased from 7.3 to 8.1. Besides the increase in peak current density, the peak of the I-V curve shifted ~5 mV in the hyperpolarizing direction when the external pH changed from 7.3 to 8.1 (see Fig. 14 *A*). No such shift was observed when internal pH changed from 7.4 to 8.1. The voltage dependence of steady state activation and inactivation of Ca^{2+} currents was determined

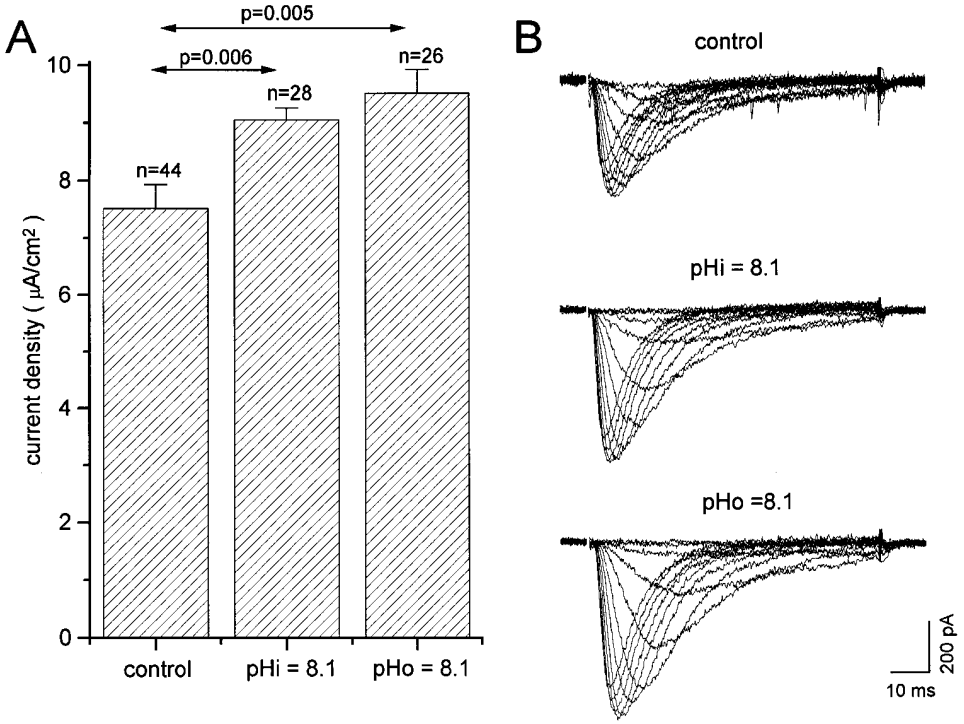

FIGURE 13. (*A*) Peak Ca^{2+} current densities obtained at two different pH_i (7.4 and 8.1), as well as at pH_o 8.1. The current density increased from 7.52 ± 0.41 to 9.06 ± 0.2 $\mu A/cm^2$ when the intracellular pH was raised from 7.4 to 8.1, and to 9.52 ± 0.41 $\mu A/cm^2$ when external pH increased from 7.3 to 8.1. The level of significance of differences between groups is indicated. (*B*) Representative Ca^{2+} current families obtained at pH_i 7.4 and 8.1 as well as at pH_o 8.1. The membrane potential was stepped (100 ms) from −70 to −15 mV in 5-mV increments. The membrane potential was held at −80 mV.

for the three experimental groups as explained in MATERIALS AND METHODS (see also Santi et al., 1996). These results are summarized in Table I. Extracellular alkalinization from pH 7.3 to 8.1 produced a 5-mV negative shift in $Va_{1/2}$ (potential of half-maximal activation). Conversely, intracellular alkalinization in the same range did not affect voltage dependence of activation or inactivation. The corresponding steepness parameters k_a and k_i remained unaffected by either external or internal alkalinization.

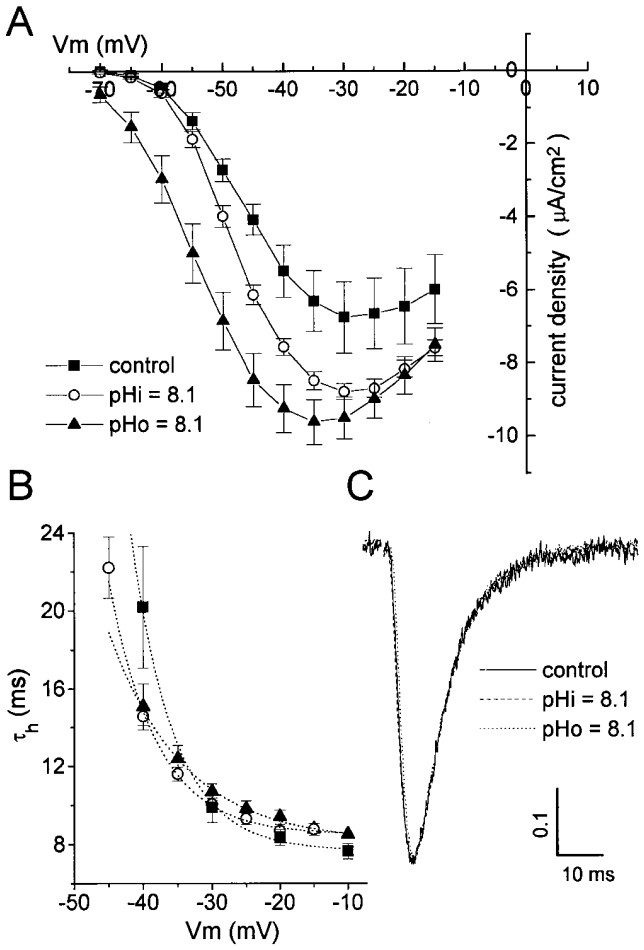

FIGURE 14. Effects of pH on current to voltage relationship of Ca^{2+} currents in primary spermatocytes. (*A*) Peak I-V relationship recorded from spermatocytes in control conditions and after increasing either internal or external pH to 8.1. (■) pH_i 7.4, (○) pH_i 8.1, (▲) pH_o 8.1. When the external pH changed from 7.3 to 8.1, the peak current density increased significantly and the I-V curve shifted 5 mV in the hyperpolarizing direction. Conversely, intracellular alkalinization increased peak current density without affecting the voltage dependence of the channels. (*B*) Voltage dependence of the time constant of inactivation (τ_h) of the decay of Ca^{2+} currents recorded under the three conditions shown in *A*. Dotted lines represent exponential fits to the data points. (*C*) Ca^{2+} current traces obtained at the peak of the I-V curves under control conditions (*continuous trace*) and after external (*dotted trace*) or internal (*dashed trace*) alkalinization to pH 8.1. Traces were normalized to their peak amplitude and superimposed for comparison. Notice that activation and inactivation kinetics of Ca^{2+} currents is not affected by alkalinization of either side of the channel.

T-type Ca^{2+} currents present in spermatogenic cells peak after a few milliseconds and decay rapidly with time courses well fitted by single exponential functions. The activation and inactivation kinetics of these currents are voltage dependent (Santi et al., 1996). To assess for possible internal and external pH effects on the voltage dependence of the rate of inactivation, Ca^{2+} records were obtained at different potentials and their time constants of inactivation (τ_h) were measured. The results are shown in Fig. 14 *B*. Data points corresponding to pH_o 8.1 were plotted with a 5-mV shift in the positive direction to compensate for the negative shift observed in the voltage dependence of the channels. As shown earlier (Santi et al., 1996), τ_h decreases markedly with depolarization, showing a strong voltage dependence in the voltage range between −45 and 0 mV. In the group of control cells, τ_h showed an *e*-fold reduction per 6.18 mV. This value was 6.86 mV for cells recorded in external medium at pH 8.1 and 10.77 mV for cells recorded with a pipette internal solution at pH 8.1. At −40 mV, the inactivation time constant of cells recorded in both external and internal alkaline solutions was significantly faster than under control conditions: 15.07 ± 1.19 ms (mean ± SEM, $n = 8$, pH_o 8.1) and 14.57 ± 0.47 ms (mean ± SEM, $n = 13$, pH_i 8.1) vs. 20.19 ± 3.12 ms (mean ± SEM, $n = 8$, control). Nevertheless, they became virtually identical at potentials positive to −30 mV regardless of the pH (see Fig. 14 *B*). This finding is further illustrated in Fig. 14 *C*, where current traces obtained at the peak of the three I-V curves shown in Fig. 14 *A* were normalized. The traces virtually superimpose onto one another. The main conclusion from this group of experiments is that the kinetics of activation and inactivation of Ca^{2+} currents are not affected to a large extent by alkalinization of either side of the channel. Thus, our data do not support the notion that, upon elevation of pH_i, the properties of T-type Ca^{2+} channels change so much as to allow sustained Ca^{2+} influx.

DISCUSSION

Intracellular pH can influence a wide variety of cellular processes (Putnam, 1995). In the adluminal compart-

TABLE I

Effects of Internal and External Alkalinization on Voltage Dependence of Activation and Steady State Inactivation of Ca^{2+} Currents

	$V_{a1/2}$	k_a	$V_{i1/2}$	k_i
	mV		*mV*	
Control	−43.66 ± 1.6	6.48 ± 0.23	−61.0 ± 2.18	5.4 ± 0.7
pH_i 8.1	−43.94 ± 0.6	6.32 ± 0.1	−58.08 ± 0.8	4.19 ± 0.27
pH_o 8.1	−48.5 ± 1.15	7.35 ± 0.3	−60.84 ± 0.96	5.08 ± 0.43

ment of seminiferous tubules, spermatogenic cells grow and differentiate in close contact and under the influence of Sertoli cells (reviewed in Jegou, 1993). Some aspects of these processes are sensitive to pH_i (Boron, 1986; Moolenaar, 1986), which is well regulated by spermatogenic cells (Osses et al., 1997). It is well established that in various systems increases in pH_i can elevate $[Ca^{2+}]_i$. Thus, one mechanism by which pH_i changes may affect differentiation is by modulating $[Ca^{2+}]_i$. In addition, elevations of pH_i modulate sperm flagellar motility in many species (Shapiro et al., 1990; Darszon et al., 1996) are required for capacitation in mammalian sperm (Meizel and Deamer, 1978; Working and Meizel, 1983; Vredenburgh and Parrish, 1995; Zeng et al., 1996) and are involved in acrosomal exocytosis in a diversity of organisms (reviewed in Darszon et al., 1996).

The information stated above suggests that a pH_i-modulated Ca^{2+} permeability pathway participates both in spermatogenesis and in sperm physiology. Since sperm are terminal cells, their ion transport systems are synthesized during spermatogenesis (Hetch, 1988). Therefore, late spermatocytes and spermatids, interesting in their own right, are good models to study the properties and regulation of ion transport systems that will be present in mature sperm (Arnoult et al., 1996*b*; Liévano et al., 1996; Santi et al., 1996). The present experiments were conducted to evaluate the influence of intracellular alkalinization on the Ca^{2+} levels in spermatogenic cells isolated from the testes of adult mice. Our results indicate that cytosolic alkalinization elicited by exposure to the cell-permeant weak base NH_4Cl increases $[Ca^{2+}]_i$ mainly by opening a plasmalemmal Ca^{2+} influx pathway. The magnitude of this response increases gradually as maturation advances, suggesting a possible role in the physiology of mature sperm. This Ca^{2+} permeation pathway allows the passage of Sr^{2+}, Ba^{2+}, and Mn^{2+} and is blocked by inorganic Ca^{2+} channel blockers Ni^{2+} and Cd^{2+}, but not by nifedipine. It is likely that, if present in mature sperm, this pH_i-regulated Ca^{2+} pathway may contribute, perhaps in concert with voltage-gated Ca^{2+} channels, to capacitation and the sustained Ca^{2+} influx required to initiate the AR.

Cytosolic pH might influence resting $[Ca^{2+}]_i$ of spermatogenic cells by way of several mechanisms. The following discussion assumes that the Ca^{2+} permeation pathway constitutes a single, elementary mechanism. Clearly, the interpretation of our results would be different if several pH-dependent processes contribute to the response.

Can pH_i Effects on Intracellular Ca^{2+} Stores Explain the Ca^{2+} Transient?

It is conceivable that upon intracellular alkalinization Ca^{2+} is released from intracellular reservoirs of spermatogenic cells. Ca^{2+}-induced Ca^{2+} release and [^{3}H]ryanodine binding is pH-sensitive, with an optimal pH in the alkaline range (>7.2; Meissner, 1994). Similarly, pH elevations enhance the rate of IP_3-induced Ca^{2+} release in skinned smooth muscle cells (Tsukioka et al., 1994). However, as shown in this study, the major source of Ca^{2+} mobilization induced by cytosolic alkalinization is plasmalemmal Ca^{2+} influx, with little or no apparent direct contribution from internal sources. In a related study (Treviño et al., 1998), we examined the density and spatial distribution of Ca^{2+} stores in primary spermatocytes and spermatids using confocal microscopy and fluorescent derivatives of thapsigargin and ryanodine. Both fluorescent analogs showed sparse but distinct labeling of endoplasmic reticulum cisternae, nuclear membrane, and Golgi complex. The scant labeling agrees with the apparently poor Ca^{2+} release that can be induced pharmacologically, suggesting that perhaps the abundance of Ca^{2+} stores is the limiting factor, rather than their filling status. These findings indicate that the amount of Ca^{2+} available for release from rapidly exchanging intracellular reservoirs in spermatogenic cells is too small to directly contribute to the Ca^{2+} signal induced by cytosolic alkalinization. Also, these results, especially those obtained with thapsigargin and cyclopiazonic acid, rule out a major role of Ca^{2+}-ATPase of endoplasmic reticulum in the generation of alkalinization-induced Ca^{2+} transients.

Proton Modulation of Plasmalemmal Voltage-gated Ca^{2+} Currents of Spermatogenic Cells

Hydrogen ions are important physiological regulators of ion flux through voltage-gated Ca^{2+} channels. As established by numerous studies, proton concentration on either side of the channel modulates L-type Ca^{2+} currents (Kaibara and Kameyama, 1988; Krafte and Kass, 1988; Klockner and Isenberg, 1994). By comparison, very little information is available on the pH modulation of T-type channels, the class of voltage-gated Ca^{2+} channels present in spermatogenic cells. In heart cells, Tytgat et al. (1990) found that external acidification reduces currents carried by T-type Ca^{2+} channels, while alkalinization enlarges them. Thus, raising pH_o from 7.4 to 8.0 increased both peak current density and maximum conductance (g_{max}) twofold. Furthermore, both the peak of the I-V curve and the half-maximal activation parameter shifted 5 mV negatively. Conversely, T-type Ca^{2+} channels were not significantly modulated by internal changes in pH in the range 6.5–8.0.

Our results with spermatogenic cells are in almost perfect agreement with those obtained in heart cells regarding external pH regulation. Also, cytosolic alkalinization slightly increased peak Ca^{2+} current density without affecting the voltage dependence of the channels. It has been shown that T-type Ca^{2+} current modulation is due to (*a*) titration of fixed surface charges near the channels, and (*b*) changes both in single chan-

nel conductance and probability of the channel being open (Tytgat et al., 1990). Given the remarkable similarities in the pH dependence of the T-type currents in heart and spermatogenic cells, it is likely that the same mechanisms are involved, although this conclusion awaits experimental confirmation. Experiments in mutated L-type Ca^{2+} channels indicate that external protons block the channel by interacting with a site along the permeation pathway rather than at an external regulatory site outside the pore (Chen et al., 1996). Since the protonation site lies within the pore, and the crucial P-region glutamates in repeats I, II, and III are perfectly conserved in all known α_1 Ca^{2+} channel subunits, it is likely that the same molecular basis underlies the pH sensitivity of T-type Ca^{2+} channels.

Can pH_i Effects on Voltage-gated Ca^{2+} Channels Explain the Ca^{2+} Transient?

Our results indicate that upon internal alkalinization both voltage dependence and kinetics of the Ca^{2+} channels remain virtually unaltered. The mild increase in peak Ca^{2+} current density upon cytosolic alkalinization could slightly augment the capability of this pathway to contribute to a sustained $[Ca^{2+}]_i$ elevation. However, external alkalinization is expected to have more repercussion, not only because it increases more Ca^{2+} current density, but also because it shifts the activation threshold to more negative potentials. In this regard, it should be stressed that, in cardiac cells, the external pH-induced changes in g_{max} showed an apparent pK_a in the range 7.1–7.5 for T-type Ca^{2+} channels, while L-type Ca^{2+} channels of the same cells had a more acidic apparent pK_a ~5.2. This difference implies that near the physiological pH, T-type Ca^{2+} channels are much more sensitive to variations in external pH than L-type Ca^{2+} channels. This divergence may be crucial in sperm, given the substantial environmental pH changes it experiences through the epididymis and during its journey along the female genital tract.

These findings, together with the inability of nifedipine to significantly inhibit alkalinization-induced Ca^{2+} transients, make unlikely that voltage-gated Ca^{2+} channels constitute a major component of the permeation pathway made available by internal alkalinization. Regardless of this conclusion, T-type Ca^{2+} channels, if present in sperm, are likely to participate in the Ca^{2+} influx required to initiate the acrosome reaction (Arnoult et al., 1996*b*; Liévano et al., 1996; Santi et al., 1996).

Can pH_i Effects on Na^+/Ca^{2+} Exchanger Explain the Ca^{2+} Transient?

It has been shown that Na^+/Ca^{2+} exchange is extremely sensitive to cytoplasmic pH, particularly in the physiological range. The activity of the exchanger is partially inhibited at physiological pH, is completely inhibited below pH 6.0, and is maximal at pH 9.0 (Doering and Lederer, 1993; Doering et al., 1996). Although external and internal pH have opposite effects on the Na^+/Ca^{2+} exchanger, its activity is about three times more sensitive to changes in pH_i than to changes in pH_o (Doering et al., 1996). Thus, under physiological conditions, where external pH changes may result in parallel pH_i changes, the inhibitory effect of H^+ is expected to dominate. Plasmalemmal Ca^{2+} influx carried by Na^+/Ca^{2+} exchange is possible under its "reverse" mode of operation (Na^+-dependent Ca^{2+} influx). This occurs when membrane potential becomes more positive than the equilibrium potential of the exchanger, $E_{Na/Ca}$. The resting membrane potential of rat spermatids in suspension has been estimated using a membrane potential sensitive dye (−22 mV; Reyes et al., 1994). The equilibrium potential of the exchanger in spermatogenic cells is not known. Nevertheless, since the resting $[Ca^{2+}]_i$ remains low and invariant for extended periods of observation (this study), it is probably safe to assume that the cell's resting potential is more negative than the exchanger's reversal potential. It could be argued that Na^+/Ca^{2+} exchange may participate in the alkalinization-induced Ca^{2+} influx based on the following similarities: (*a*) the Na^+/Ca^{2+} activity increases upon cytosolic alkalinization (see above); (*b*) Sr^{2+} and Ba^{2+} can also be transported by the exchanger, thus allowing these divalents to enter the cell (Tibbits and Philipson, 1985; Condrescu et al., 1997); (*c*) Ni^{2+} inhibits the Na^+/Ca^{2+} exchanger at low millimolar concentrations, but not nifedipine (Trosper and Philipson, 1983); and (*d*) monensin, which enhances alkalinization-induced responses, also stimulates the reverse mode of operation of the Na^+/Ca^{2+} exchange by increasing $[Na^+]_i$ (Santi et al., 1995).

In spite of these similarities, alkalinization-induced Ca^{2+} entry differs from Na^+/Ca^{2+} exchange in several crucial aspects. First, the former readily allows Mn^{2+} influx, while the exchanger cannot transport this divalent (Trosper and Philipson, 1983). Furthermore, superfusion with 10 μM 2-4 dichlorobenzamil, a relatively specific inhibitor of the Na^+/Ca^{2+} exchanger, does not suppress alkalinization-induced Ca^{2+} transients (data not shown). Finally, ouabain (30 μM) does not enhance alkalinization-induced Ca^{2+} transients even though, like monensin, it increases $[Na^+]_i$ by inhibiting the Na^+/K^+-ATPase (data not shown). These findings are inconsistent with a significant participation of the Na^+/Ca^{2+} exchanger in the pH-dependent Ca^{2+} entry of spermatogenic cells.

Can Effects on other Ca^{2+} Entry Pathways Account for the Alkalinization-induced Ca^{2+} Transient?

In nonexcitable cells, intracellular calcium release is followed by a sustained "store-operated Ca^{2+} influx"

(Putney, 1986, 1997; reviewed in Parekh and Penner, 1997). The associated inward currents, termed I_{CRAC} (calcium-release activated currents) or I_{SOC} (store operated channel) are highly selective for Ca^{2+} over monovalents (Hoth and Penner, 1993; Yao and Tsien, 1997). Another calcium entry pathway, clearly distinct from I_{CRAC} exists in some cell types (Putney, 1997), and could correspond to $InsP_3$ receptors present in the plasma membrane (Vaca and Kunze, 1995). The properties of these Ca^{2+} entry mechanisms resemble those of the alkalinization-induced Ca^{2+} influx pathway: I_{CRAC} and I_{SOC} display high selectivity for Ca^{2+} ions, although other divalents, such as Ba^{2+} and Sr^{2+}, are also permeant (Hoth and Penner, 1993; Yao and Tsien, 1997). Ni^{2+} and Cd^{2+} block both currents (Premack et al., 1994; Zweifach and Lewis, 1993; Yao and Tsien, 1997). Similarly, the $InsP_3$-induced permeation across the plasma membrane of Jurkat T cells has relative cation conductances $Ca^{2+} > Ba^{2+} > Sr^{2+}$, and La^{3+} and Cd^{2+} have been used as nonspecific blockers of $InsP_3$ receptors. Both I_{CRAC} and $InsP_3$ receptors, although Ca^{2+} selective, allow the passage of Mn^{2+} (Fasolato et al., 1993; Hoth and Penner, 1993; Premack et al., 1994; Zweifach and Lewis, 1993). Interestingly, pH is an important modulator of the activity of both mechanisms (Tsukioka et al., 1994; Iwasawa et al., 1997).

As shown earlier, Ca^{2+} release from internal stores does not play a major role in directly generating the alkalinization-induced Ca^{2+} transients in spermatogenic cells, probably because their Ca^{2+} stores are not very abundant. Nonetheless, these findings do not rule out the possibility that pH-induced depletion of Ca^{2+} stores may lead to opening of SOCs. Since the activity of this Ca^{2+} influx pathway is itself regulated by intracellular pH, it is conceivable that it could participate or even be responsible for the alkalinization-induced Ca^{2+} rise.

The expression of SOCs in spermatogenic cells has not been thoroughly examined. Nevertheless, the experiments shown in Fig. 9 *E*, and particularly those in Fig. 10, are consistent with the presence of such channels. The slow and sustained Ca^{2+} influx observed upon the readmission of external Ca^{2+} after thapsigargin application indicates that spermatogenic cells contain thapsigargin-sensitive sarcoplasmic/endoplasmic reticulum Ca^{2+}-ATPases. The absence of a significant Ca^{2+} rise during thapsigargin application could be due to the presence of a mechanism that extrudes Ca^{2+} as quickly as it is released. Secondly, these experiments strongly suggest that spermatogenic cells express SOCs. It remains to be explored if this Ca^{2+} permeation pathway is responsible for the alkalinization-induced Ca^{2+} entry. Alternatively, this route could represent a novel pH-regulated channel, predominantly expressed in late spermatogenic cells, not unlike Slo3, a novel potassium channel abundantly expressed in mammalian spermatocytes and regulated by both intracellular pH and membrane voltage (Schreiber et al., 1998).

Possible Functional Significance of the Alkalinization-induced Ca^{2+} Transients in Mature Sperm Physiology

As shown here, testicular sperm undergo large $[Ca^{2+}]_i$ increases when exposed to NH_4Cl. In this regard, it is worth considering how a pH_i-dependent Ca^{2+} permeability pathway could influence sperm physiology.

Sperm travel through very different environments in an excursion that lasts many days from the seminiferous tubules to the oviduct. Clearly, environmental changes, pH_o among them, can influence their physiological state and rate of survival. These changes select the fittest sperm and induce the maturation processes required to achieve fertilization at the appropriate site (reviewed in Harper, 1988; Setchell and Brooks, 1988). In this context, it is not difficult to imagine that the pH-dependent Ca^{2+} permeability pathway described here, along with T-type Ca^{2+} channels, which are also sensitive to external pH, may modulate $[Ca^{2+}]_i$, thus influencing sperm function along the tortuous path towards the egg.

Before they can acquire the capacity to fertilize the egg, sperm need to become capacitated, a process that involves a series of ill defined functional and biophysical modifications (Florman and Babcock, 1991; Baldi et al., 1996). An obligatory step during in vitro capacitation is internal alkalinization from pH ~6.5 to 6.7 (Parrish et al., 1989; Zeng et al., 1996; reviewed in Baldi et al., 1996). Interestingly, this is the same range of pH change required for spermatogenic cells to respond to alkalinization with Ca^{2+} rises. It can be speculated that the "pH threshold" phenomenon, along with the use-dependent facilitation here described, is relevant for the mechanism of capacitation by allowing cells to respond more vigorously to subsequent episodes of intracellular alkalinization.

Several models exist to explain the sperm AR, a Ca^{2+}-dependent exocytotic event required for fertilization, but the precise order of events and the molecular identity of the participants remains elusive (Arnoult et al., 1996*a*; Darszon et al., 1996). In a striking similarity to sea urchin sperm (Guerrero and Darszon, 1989*a*, 1989*b*), at least two different Ca^{2+} channels are believed to participate in the mammalian sperm AR (Florman, 1994, Tiwari-Woodruff et al., 1995). It has been proposed (Arnoult et al., 1996*a*) that a cation channel that allows Ca^{2+} influx depolarizes the spermatozoon, thus opening T-type Ca^{2+} channels (Arnoult et al., 1996*b*; Liévano et al., 1996; Santi et al., 1996). The ensuing Ca^{2+} rise, together with the pH_i increase, would trigger the AR. One problem with this model is that Ca^{2+} channels only activate transiently, thus precluding

sustained $[Ca^{2+}]_i$ elevations. As shown here, this shortcoming of the voltage-gated pathway is not lessened by internal alkalinization. On the other hand, the pH_i-regulated Ca^{2+} pathway described here appears more suitable for supporting sustained Ca^{2+} elevations.

Sperm are devoted to the generation of a new individual. An exquisitely choreographed signaling cascade is required to reach this goal, which may use specific ion-transport variations not evident in other cell types. This novel pH-dependent Ca^{2+} permeation pathway, assuming its presence in mature sperm, could be one of the ion-transport variations responsible for the dihydropyridine-insensitive Ca^{2+} influx that precedes and triggers the acrosome reaction.

The authors thank Drs. Agustín Guerrero and Javier Alvarez-Leefmans for many useful discussions, and Drs. Larry Salkoff and Luis Vaca for reviewing an earlier version of this manuscript. Dr. Reinaldo Dipolo made many helpful suggestions in the early stages of this project. We also thank Dr. José Luis Molinari for providing healthy mice from his colony and Nicolás Jiménez for help in conducting some experiments.

This work was supported by grants from DGAPA-UNAM (IN206395, IN204497) and CONACyT (2366PN, 25261-N; México) to A. Hernández-Cruz, and by the Howard Hughes Medical Institute and the International Centre for Genetic Engineering and Biotechnology to A. Darszon. This work was conducted by C.M. Santi in partial fulfillment of her Ph.D. Thesis. For that purpose, she was awarded a Ph.D. fellowship from DGAPA-UNAM.

Original version received 8 April 1998 and accepted version received 7 May 1998.

REFERENCES

Arnoult, C., Y. Zeng, and H.M. Florman. 1996*a*. ZP3-dependent activation of sperm cation channels regulates acrosomal secretion during mammalian fertilization. *J. Cell Biol.* 134:637–645.

Arnoult, C., R.A. Cardullo, J.R. Lemos, and H.M. Florman. 1996*b*. Activation of mouse sperm T-type Ca^{2+} channels by adhesion to the egg zona pellucida. *Proc. Natl. Acad. Sci. USA.* 93:13004–13009.

Arnoult, C., J.R. Lemos, and H.M. Florman. 1997. Voltage-dependent modulation of T-type calcium channels by protein tyrosine phosphorylation. *EMBO (Eur. Mol. Biol. Organ.) J.* 16:1593–1599.

Babcock, D.F., and D.R. Pfeiffer. 1987. Independent elevation of cytosolic $[Ca^{2+}]$ and pH of mammalian sperm by voltage dependent and pH-sensitive mechanisms. *J. Biol. Chem.* 262:15041–15047.

Baldi, E., L. Michaela, L. Bonaccorsi, C. Krausz, and G. Forti. 1996. Human sperm activation during capacitation and acrosome reaction: role of calcium, protein phosphorylation and lipid remodeling pathways. *Front. Biosci.* 1:189–205.

Batlle, D., C.R. Peces, M.S. LaPointe, M. Ye, and J.T. Daugirdas. 1993. Cytosolic free calcium regulation in response to acute changes in intracellular pH in vascular smooth muscle. *Am. J. Physiol.* 264:C932–C943.

Bellvé, A.R., C.F. Millette, Y.M. Bhatnagar, and D.A. O'Brien. 1977. Dissociation of the mouse testis and characterization of isolated spermatogenic cells. *J. Histochem. Cytochem.* 25:480–494.

Beltrán, C., O. Zapata, and A. Darszon. 1996. Membrane potential regulates sea urchin sperm adenylcyclase. *Biochemistry.* 35:7591–7598.

Benning, N., J. Leipsinger, R. Greger, and R. Nitschke. 1996. Effects of alkalinization of cytosolic pH by amines on intracellular Ca^{2+} activity in HT29 cells. *Pflügers Arch.* 432:126–133.

Bevensee, M.O., and W.F. Boron. 1995. Manipulation and regulation of cytosolic pH. *In* Methods in Neurosciences. Vol. 27. Academic Press Inc., Orlando, FL. 252–272.

Boron, W.F. 1986. Special topic: acid/base physiology. *Annu. Rev. Physiol.* 48:347–413.

Chen, X.-H., I. Bezprozvanny, and R.W. Tsien. 1996. Molecular basis for proton block of L-type Ca^{2+} channels. *J. Gen. Physiol.* 108: 363–374.

Condrescu, M., G. Chernaya, V. Kalaria, and J.P. Reeves. 1997. Barium influx mediated by the cardiac sodium-calcium exchanger in transfected chinese hamster ovary cells. *J. Gen. Physiol.* 109:41–51.

Danthuluri, N.R., D. Kim, and T.A. Brock. 1990. Intracellular alkalinization leads to Ca^{2+} mobilization from agonist-sensitive pools in bovine aortic endothelial cells. *J. Biol. Chem.* 265:19071–19076.

Darszon, A., A. Liévano, and C. Beltrán. 1996. Ion channels: key elements in gamete signaling. *Curr. Top. Dev. Biol.* 34:117–167.

Dickens, C.J., J.I. Gillespie, J.R. Greenwell, and P. Hutchinson. 1990. Relationship between intracellular pH (pH_i) and calcium $(Ca^{2+})i$ in avian heart fibroblasts. *Exp. Cell. Res.* 187:39–46.

Doering, A.E., and W.J. Lederer. 1993. The mechanism by which cytoplasmic protons inhibit the sodium-calcium exchanger in guinea-pig heart cells. *J. Physiol. (Camb.).* 466:481–499.

Doering, A.E., D.A. Eisner, and W.J. Lederer. 1996. Cardiac Na-Ca exchange and pH. *Ann. NY Acad. Sci.* 779:182–198.

Fasolato, C., M. Hoth, and R. Penner. 1993. Multiple mechanisms of manganese-induced quenching of fura-2 fluorescence in rat mast cells. *Pflügers. Arch.* 423:225–231.

Florman, H.M., R.M. Tombes, N.L. First, and D.F. Babcock. 1989. An adhesion-associated agonist from the zona pellucida activates G protein-promoted elevations of internal Ca^{2+} and pH that mediate mammalian sperm acrosomal exocytosis. *Dev. Biol.* 135:133–146.

Florman, H.M., and D.F. Babcock. 1991. Progress toward understanding the molecular basis of capacitation. *In* Elements of Mammalian Fertilization. I. Basic concepts. P.M. Wassermann, editor. CRC Press, Boca Raton, FL. 105–132.

Florman, H.M, M.E. Corron, T.D.-H. Kim, and D.F. Babcock. 1992. Activation of voltage-dependent calcium channels of mammalian sperm is required for zona pellucida-induced acrosomal exocytosis. *Dev. Biol.* 152:304–314.

Florman, H.M. 1994. Sequential focal and global elevations of sperm intracellular Ca^{2+} are initiated by the zona pellucida during acrosomal exocytosis. *Dev. Biol.* 165:152–164.

Gabers, D.L. 1989. Molecular basis of fertilization. *Annu. Rev. Biochem.* 58:719–742.

García-Soto, J., M. González-Martínez, L. De la Torre, and A. Darszon. 1987. Internal pH can regulate Ca^{2+} uptake and the acrosome reaction in sea urchin sperm. *Dev. Biol.* 120:112–120.

Grinstein, S., and J.D. Goetz. 1985. Control of free cytoplasmic calcium by intracellular pH in rat lymphocytes. *Biochim. Biophys. Acta.* 819:267–270.

Grynkiewicz, G., M. Poenie, and R.Y. Tsien. 1985. A new generation

of Ca^{2+} indicators with greatly improved fluorescence properties. *J. Biol. Chem.* 260:3440–3450.

Guerrero, A., and A. Darszon. 1989*a*. Egg jelly triggers a calcium influx which inactivates and is inhibited by calmodulin antagonists in the sea urchin sperm. *Biochim. Biophys. Acta.* 980:109–116.

Guerrero, A., and A. Darszon. 1989*b*. Evidence for the activation of two different Ca^{2+} channels during the egg jelly induced acrosome reaction of sea urchin sperm. *J. Biol. Chem.* 264:19593–19599.

Harper, M.J.K. 1988. Gamete and zygote transport. *In* The Physiology of Reproduction. Vol. 1. E. Knobil and J.D. Neill, editors. Raven Press, New York. 103–134.

Hernández-Cruz, A., A.L. Escobar, and N. Jiménez. 1997. Ca^{2+}-induced Ca^{2+} release phenomena in mammalian sympathetic neurons are critically dependent on the rate of rise of trigger Ca^{2+}. *J. Gen. Physiol.* 109:147–167.

Hetch, N.B. 1988. Post meiotic gene expression during spermatogenesis. *In* Meiotic Inhibition: Molecular Control of Meiosis. Vol. 267. F.P. Haseltine and N.L. First, editors. Alan R. Liss, New York. 291 pp.

Hoth, M., and R. Penner. 1993. Calcium release-activated calcium current in rat mast cells. *J. Physiol. (Camb.).* 465:359–386.

Iwasawa, K., T. Nakajima, H. Hazama, A. Goto, W.-S. Shin, T. Toyooka, and M. Omata. 1997. Effects of extracellular pH on receptor-mediated Ca^{2+} influx in A7r5 rat smooth muscle cells: involvement of two different types of channel. *J. Physiol. (Camb.).* 503:237–251.

Jegou, B. 1993. The sertoli-germ cell communication network in mammals. *Int. Rev. Cytol.* 147:25–96.

Kaibara, M., and M. Kameyama. 1988. Inhibition of the calcium channel by intracellular protons in single ventricular myocytes of the guinea-pig. *J. Physiol. (Camb.).* 403:621–640.

Klockner, U., and G. Isenberg. 1994. Calcium channel current of vascular smooth muscle cells: extracellular protons modulate gating and single channel conductance. *J. Gen. Physiol.* 103:665–678.

Konishi, M., A. Olson, S. Hollingworth, and S.M. Baylor. 1988. Myoplasmic binding of fura-2 investigated by steady-state fluorescence and absorbance measurements. *Biophys. J.* 54:1089–1104.

Krafte, D.S., and R.S. Kass. 1988. Hydrogen ion modulation of Ca^{2+} channels current in cardiac ventricular cells. *J. Gen. Physiol.* 91: 641–657.

Liévano, A., C.M. Santi, C.J. Serrano, C.L. Treviño, A.R. Bellvé, A. Hernández-Cruz, and A. Darszon. 1996. T-type Ca^{2+} channels and α_{1E} expression in spermatogenic cells, and their possible relevance to the sperm acrosome reaction. *FEBS Lett.* 388:150–154.

Martínez-Zaguilán, R., G.M. Martínez, F. Lattanzio, and R.J. Gillies. 1991. Simultaneous measurement of intracellular pH and Ca^{2+} using the fluorescence of SNARF-1 and Fura-2. *Am. J. Physiol.* 260: C297–C307.

Martínez-Zaguilán, R., M.W. Gurulé, and R.M. Lynch. 1996. Simultaneous measurement of intracellular pH and Ca^{2+} in insulin secreting cells by spectral imaging microscopy. *Am. J. Physiol.* 270: C1438–C1446.

Meissner, G. 1994. Ryanodine receptor/Ca^{2+} release channels and their regulation by endogenous effectors. *Annu. Rev. Physiol.* 56: 485–508.

Meizel, S., and D.W. Deamer. 1978. The pH of the hamster sperm acrosome. *J. Histochem. Cytochem.* 26:98–105.

Moolenaar, W.H. 1986. Effects of growth factors on intracellular pH regulation. *Annu. Rev. Physiol.* 48:363–376.

Nitschke, R., A. Riedel, S. Ricken, J. Leipziger, N. Benning, K.-G. Fischer, and R. Greger. 1996. The effect of intracellular pH on cytosolic Ca^{2+} in HT_{29} cells. *Eur. J. Physiol.* 433:98–108.

Osses, N., F. Pancetti, D.J. Benos, and J.G. Reyes. 1997. Intracellular pH regulation in rat spermatids. *Biol. Cell.* 89:273–283.

Parekh, A.B., and R. Penner. 1997. Store depletion and calcium influx. *Physiol. Rev.* 77:901–930.

Parish, J.J., J.L. Susko-Parish, and N.L. First. 1989. Capacitation of bovine sperm by heparin: inhibitory effect of glucose and role of intracellular pH. *Biol. Reprod.* 49:683–699.

Premack, B.A., T.V. McDonald, and P. Gardner. 1994. Activation of a Ca^{2+} current in Jurkat T cells following the depletion of Ca^{2+} stores by microsomal Ca^{2+}-ATPase inhibitors. *J. Immunol.* 152: 5226–5240.

Putnam, R.W. 1995. Intracellular pH regulation. *In* Cell Physiology. N.D. Speralakis, editor. Academic Press, New York. 212–229.

Putney, J.W., Jr. 1986. A model for receptor regulated calcium entry. *Cell Calc.* 7:1–12.

Putney, J.W., Jr. 1997. Type 3 inositol 1,4,5-trisphosphate receptor and capacitative calcium entry. *Cell Calc.* 21:257–261.

Reyes, J.G., J. Bacigalupo, R. Araya, and D.J. Benos. 1994. Ion dependence of resting membrane potential of rat spermatids. *J. Reprod. Fert.* 102:313–319.

Santi, C.M., J.A. Connor, and A. Hernández-Cruz. 1995. A significant fraction of calcium transients in intact guinea pig ventricular myocytes is mediated by Na^+-Ca^{2+} exchange. *Cell. Signal.* 7:803–820.

Santi, C.M., A. Darszon, and A. Hernández-Cruz. 1996. A dihydropyridine-sensitive T-type Ca^{2+} current is the main Ca^{2+} current carrier in mouse primary spermatocytes. *Am. J. Physiol.* 271: C1583–C1593.

Setchell, B.P., and D.E. Brooks. 1988. Anatomy, vasculature, innervation, and fluids of the male reproductive tract. *In* The Physiology of Reproduction. Vol. 1. E. Knobil and J.D. Neill, editors. Raven Press, New York. 933–974.

Schreiber, M., A. Wei, A. Yuan, J. Gaut, M. Saito, and L. Salkoff. 1998. Slo3, a novel pH-sensitive K^+ channel from mammalian spermatocytes. *J. Biol. Chem.* 273:3509–3516.

Shapiro, B.M., S. Cook, A.F.G. Quest, J. Oberdorf, and D. Wothe. 1990. Molecular mechanisms of sea urchin-sperm activation before fertilization. *J. Reprod. Fert. (Suppl.).* 42:3–8.

Shorte, S.L., G.L. Collingridge, A.D. Randall, J.B. Chappell, and J.G. Schofield. 1991. Ammonium ions mobilize calcium from an internal pool which is sensitive to TRH and ionomycin in bovine anterior pituitary cells. *Cell Calc.* 12:301–312.

Siskind, M.S., C.E. McCoy, A. Chobanian, and J.H. Schwartz. 1989. Regulation of intracellular calcium by pH in vascular smooth muscle cells. *Am. J. Physiol.* 256:C234–C240.

Tajima, Y., N. Okamura, and Y. Sugita. 1987. The activating effects of bicarbonate on sperm motility and respiration at ejaculation. *Biochim. Biophys. Acta.* 924:519.

Tibbits, G.F., and K.D. Philipson. 1985. Na^+-dependent alkaline earth metal uptake in cardiac sarcolemmal vesicles. *Biochim. Biophys. Acta.* 817:327–332.

Tiwari-Woodruff, S.K., and T.C. Cox. 1995. Boar sperm plasma membrane Ca^{2+}-selective channels in planar lipid bilayers. *Am. J. Physiol.* 265:C1284–C1294.

Treviño, C.L., C.M. Santi, C. Beltrán, A. Hernández-Cruz, A. Darszon, and H. Lomelí. 1998. Localization of IP_3 and ryanodine receptors during mouse spermatogenesis: possible functional implications. *Zygote.* In press.

Trimmer, J.S., and V.D. Vacquier. 1986. Activation of sea urchin gametes. *Annu. Rev. Cell Biol.* 2:1–26.

Trosper, T.L., and K.D. Philipson. 1983. Effects of divalent and trivalent cations on Na^+/Ca^{2+} exchange in cardiac sarcolemmal vesicles. *Biochim. Biophys. Acta.* 731:63–68.

Tsukioka, M., M. Iino, and M. Endo. 1994. pH dependence of inositol-1,4,5-trisphosphate-induced Ca^{2+} release from permeabilized smooth muscle cells of the guinea-pig. *J. Physiol. (Camb.).* 475: 369–375.

Tytgat, J., B. Nilius, and E. Carmeliet. 1990. Modulation of T-type

cardiac Ca channel by changes in proton concentration. *J. Gen. Physiol.* 96:973–990.

Vaca, L., and D.L. Kunze. 1995. IP_3-activated Ca^{2+} channels in the plasma membrane of cultured vascular endothelial cells. *Am. J. Physiol.* 269:C733–C738.

Vredenburgh, W.L., and J.J. Parrish. 1995. Intracellular pH of bovine sperm increases during capacitation. *Mol. Reprod. Dev.* 40: 490–502.

Wiegmann, T.B., L.W. Welling, D.M. Beatty, D.E. Howard, S. Vamos, and S.J. Morris. 1993. Simultaneous imaging of intracellular $[Ca^{2+}]_i$ and pH in single MDCK and glomerular epithelial cells. *Am. J. Physiol.* 265:C1184–C1190.

Working, P.K., and S. Meizel. 1983. Correlation of increased intraacrosomal pH with the hamster sperm acrosome reaction. *J. Exp. Zool.* 227:97–107.

Yao, Y., and R.Y. Tsien. 1997. Calcium current activated by depletion of calcium stores in *Xenopus* oocytes. *J. Gen. Physiol.* 109:703–715.

Yodozawa, S., T. Speake, and A. Elliott. 1997. Intracellular alkalinization mobilizes calcium from agonist-sensitive pools in rat lachrymal acinar cells. *J. Physiol. (Camb.).* 499:601–611.

Zeng, Y., J.A. Oberdorf, and H.M. Florman. 1996. pH regulation in mouse sperm: identification of Na^+-, Cl^--, and $HCO3^-$-dependent and arylaminobenzoate-dependent regulatory mechanisms and characterization of their roles in sperm capacitation. *Dev. Biol.* 173:510–520.

Zweifach, A., and R.S. Lewis. 1993. Mitogen-regulated Ca^{2+} current in T lymphocytes is activated by depletion of intracellular Ca^{2+} stores. *Proc. Natl. Acad. Sci. USA.* 90:6295–6299.